DOCTORAL THESIS

Gametogenesis and flower development controlled by AtAnamorsin1 and AtPUB4

Yu, Boying

Date of Award:
2015

Gametogenesis and Flower Development Controlled by AtAnamorsin1 and AtPUB4

YU Boying

A thesis submitted in partial fulfilment of the requirements

for the degree of

Doctor of Physiology

Principal Supervisor: Prof. XIA Yiji

Hong Kong Baptist University

January 2015

Declaration

I hereby declare that this thesis represents my own work which has been done after registration for the degree of Ph.D at Hong Kong Baptist University, and has not been previously included in a thesis, dissertation submitted to this or other institution for a degree, diploma or other qualification.

Signature: _____

Date: January 2015

Abstract

Flowers are the organs for sexual reproduction in angiosperms. Gametogenesis in floral organs leads to formation of sperms and eggs and their fertilization forms a zygote that develops into a new plant. Gametogenesis and embryogenesis involve precisely regulated biological processes controlled by complex networks of genes and pathways.

In this study, AtANA1, which was identified as a redox sensitive protein in previous study, was found to be essential for embryogenesis and also plays an important role in both male and female gametogenesis. Without a functional AtANA1, embryo development is arrested after the first cell division of the zygote. The ana1 mutation also causes arrest in different steps of male and female gametogenesis. Aborting pollen and embryos caused by the ana1 mutation exhibit enhanced accumulation of reactive oxygen species and DNA fragmentation, marks of programmed cell death. Presence of aborting *ana1* pollen was also found to lead to abortion of wild type pollen in the same anther, raising a possibility that the aborting ana1 pollen might release a death signal. ANA1 could be involved in an oxidative stress signaling pathway, and loss of its function triggers death of gametophytic and embryonic cells.

Another important protein involved in Arabidopsis reproductive processes is PUB4, an E3 ubiquitin ligase. The *pub4* mutation was previously found to cause abnormal enlargement of tapetal cells and incomplete degeneration of the tapetum layer, resulting in a defect in pollen release and conditional male sterility. In this study, we characterized PUB4's role in controlling floral meristem determinacy. The *pub4* mutation causes formation of ectopic floral organs inside of carpels/siliques. It was found that the *pub4* mutation leads to ectopic expression of *WUSCHEL*, an important regulator which is essential for maintaining shoot apical meristem and floral meristem, which could be responsible for the flower-in-flower phenotype. PUB4 appears to work additively with AGAMOUS (AG) to control appropriate expression of the *WUS* gene. Three extra large G proteins (XLGs) in *Arabidopsis*, which interact with PUB4, also play roles in controlling tapetal cell enlargement and degeneration. However, XLGs might not function in floral meristem determinacy.

Acknowledgements

Foremost, I would like to show my sincere gratitude to my principal supervisor, Prof Xia Yiji, for his fully support, every enlightened suggestion, and encouragement during my study period. Without his guidance, his patience, and his immense knowledge, I would never have finished my study and completed this thesis. I could not imagine a better mentor for my Ph.D study.

I also want to thank Dr. QIU Jianwen, and Prof. ZHANG Jianhua for their precious comments and constant help in these years.

I am also grateful to my laboratory technician, Ms. Louise Ng Lai Ha, for her technical supports, experiment materials and chemicals ordering. Besides, I also want to show my thanks to technicians of our department, Mr. Ip Wang Kwong, and Mr. Chung Wai Shing, for teaching me detail research skills. I want to thank the secretary of our department, Ms Lau Pui Ling, and executive assistant in graduate school, Mr. K.F. Lo, for their generous help every time.

In addition, my great thanks goes to our lab members: Yin Zhao, Liu Pei, Wang Yipin, Wu Yingying, Jiang Tiantian, Yu peipei, Li yimim, Zhang Hailei for their help, for the friendship, for their company through the past four years.

Last not but least, I would like to express my thanks to my family members for their spiritually support and encouragements during my whole study period.

Table of Contents

List of the Tables

List of the Figures

List of Abbreviations

AG	AGAMOUS
AP	APETALA
ANA1	AtANAMORSIN1
APC/C	anaphase-promoting complex/ cyclosome
ARF-GEF	GDP/GTP exchange factor for small G proteins of the ARF
ASY1	ASYNAPTIC1
BDL	BODENLOS
BLR	BELLRINGER
BP	BREVIPEDICELLUS
BR	brassinosteroid
CAL	CAULIFLOWER
CAN	CORONA
CIAPIN1	cytokine-induced apoptosis inhibitor 1
CK	cytokinins
CLV	CLAVATA
Col	Columbia
CTAB	Cetyltrimethyl ammonium bromide
CUC	CUP-SHAPED COTYLEDON1
CZ	central zone
DAB	3,3'-Diaminobenzidine
DAPI	4',6-diamidino-2-phenylindole

DIC	differential interference contrast
DIF1	DETERMINATE INFERTILE1
DME	Demeter
duo	duo pollen
DYT	double-yeast-tryptone medium
E1	ubiquitin activity enzyme
E2	ubiquitin conjugating enzyme
E3	ubiquitin protein ligase
FBL17	F-box-Like 17
FER	FERONIA
FM	floral meristem
FT	FLOWER TIMING
GA	gibberellin
GEM	*gemini pollen*
GEX3	GAMETE EXPRESSED3
GST	glutathioneS-transferase
GUS	β-Glucuronidase
HD-ZIPIII	homeodomain leucine zipper family
IAF	thiols by 5-iodoacetamidofluorescein
IM	inflorescence meristem
IPT	isopentenyl transferases
KNAT	knotted1-like homeobox

KNOX	knotted1-like homeobox
KNU	KNUCKLES
LFY	LEAFY
Lug	LEUNIG
MP	MONOPTEROS
NDK2	NUCLEOTIDE DIPHOSPHATE KINASE2
NZZ	NOZZLE
OC	organizing center
PCD	Program cell death
PHB	PHABULOSA
PHV	PHAVOLUTA
PI	PISTILLATA
PI	Propidium iodide
PIN7	PIN-FORMED 7
PLL1	POL1-LIKE1
PMI	Pollen Mitosis I
PMII	pollen mitosis II
POL1	POLTERGEIST
PUB4	Plant-U-Box
PZ	peripheral zone
qrt	quartet
RAM	root apical meristem

RBR	RETINO BLASTOMA RELATED
REV	REVOLUTA
ROS	reactive oxygen species
RPT	Regulatory Particle Triple A ATPase
RZ	rib zone
SAM	shoot apical meristem
SCP	SIDECAR POLLEN
SEP	SEPALLATA
SEU	SEUSS
SPL	SPOROCYTELESS
STIP	STIMPY
STM	SHOOT MERISTEMLESS
SUP	SUPERMAN
TFL	TERMINAL FLOWER
TUNEL	Terminal Deoxynucleotidyl Transferase dUTP Nick End Labeling
UFO	UNSUAL FLORAL ORGANS
ULT1	ULTRAPETALA1
WOX	WUSCHEL RELATED HOMEOBOX
WRKY	WRKY DNA-BINDING PROTEIN 2
WT	wild type
WUS	WUSCHEL
XLG	Extra-Large G protein

ZPR	LITTLE ZIPPER

Chapter One - Literature Review

1.1 The Shoot Apical Meristem

1.1.1 Introduction to the shoot apical meristem

Development of plant begins from the shoot apical meristem (SAM), which continuously generates organs and tissues. Different organs, such as leaves, stems and flowers, are originally produced from the SAM. The SAM consists of around 500 cells and is divided into three cell layers (L1-3). L1 is formed from cells at tip of the apex, which divide in anticlinal plane and will develop into epidermis. Cells belonging to L2 also divide in anticlinal plane and will form into mesophyll cells. Cells in L3 can divide both anticlinally and periclinally and form central tissues of leaves and stems. These cell layers can be also classified into zones through function and cytohistology. The central zone (CZ) contains pluripotent stem cells and locates at middle of the SAM. The cells in the peripheral zone (PZ) will differentiate into lateral organs. And the rib zone (RZ) locating inside of CZ plays a role in supporting the SAM by differentiation of multipotent cells into stems (Dodsworth, 2009).

1.1.2 Signalling pathways in the SAM

Regulators involved in SAM maintenance always relate to the signaling network of WUSCHEL (WUS). *WUS* is expressed by a pile of cells in organizing center (OC), which locates under the stem cell at the central of L3. *WUS*, belonging to the *WUSCHEL RELATED HOMEOBOX* (WOX) gene family, encodes a

transcription factor and promotes stem cells activity. This point of view is proved by the *wus* mutant, whose stem cells fail to produce a shoot meristem in the embryo and are consumed by developing organ primordia (Laux et al., 1996). Regulations of *WUS* expression were described by various reports. Among them, CLAVATA (CLV)-WUS feedback loop is one of the most important and notable signaling pathways. Expression of *WUS* provides signals to stimulate expression of *CLV3*. *CLV3*, in turn, forms a negative feedback loop to *WUS* and represses expression of *WUS*. CLV3 is originally expressed in L1 and L2 layers and moves to the inner layer through a receptor consisting of CLV1 and ClV2 polypeptides. Mutations of any CLVs will cause elevated expression of *WUS* and result in enlarged CZ. *WUS* utilizes CLV3 to control its expression level and maintain meristem size (Schoof H et al., 2000; Dievart, 2003). Downstream proteins of CLV3 are also considered to be involved in this feedback loop, such as phosphatases, POLTERGEIST (POL1) and POL1-LIKE1 (PLL1). Mutation of POL1 and PLL2 suppresses phenotypes of *clv1*, *clv2*, and *clv3*. Besides, overexpression of POL1 and PLL2 in the *clv* mutants results in exacerbated phenotype of the *clv* mutants (Yu et al., 2000; Yu et al., 2003).

Besides the CLV-WUS feedback pathway, there are many regulators also controlling expression of *WUS*. The positive regulator, STIMPY (STIP or WOX9) is considered as a WUS-related homeobox transcription factor. Mutation of the *STIP* impairs formation of the SAM and disrupts expression of *WUS* and *CLV*. The *STIP* mutation suppresses phenotype of *clv3* and its overexpression enhances

the *clv3* phenotype. Thus, *STIP* is considered to be a positive regulator of *WUS* and a negative regulator of *CLV3* (Wu et al., 2005). The *APETALA* (*AP2*), the A function gene in ABC model of floral development, is also considered to be a positive regulator of the *WUS* gen and a negative regulator of the *CLV* gene. Mutation of *AP2* shows similar phenotype of the *wus* mutant (Wurschum et al., 2006).

ULTRAPETALA1 (ULT1), a SAND-domain transcription factor, negatively regulates expression of *WUS* during later stages of floral development. Mutation of *ULT1* causes enlarged inflorescences and floral meristem. Double mutant of the *ULT1* gene and the *CLV* gene resulted in enhanced phenotype (Carles et al., 2005). Five class III genes belonging to homeodomain leucine zipper family (HD-ZIPIII), the *CORONA* (*CNA*), the *PHABULOSA* (*PHB*), the *PHAVOLUTA* (*PHV*), the *REVOLUTA* (*REV*) and the *ATHB8*, down regulate *WUS* transcription and confine expression of *WUS*. Triple mutations of them cause enlargement of SAM. The miRNA 165/166 are also considered to regulate *WUS* through regulating the five HD-ZIP III genes by cleavage of their mRNAs. Besides of miRNA165/166, LITTLE ZIPPER proteins (ZPR) also negatively regulate five HD-ZIP III genes expression (Williams et al., 2005). ZPR3 was proved to form inactive heterodimers with HD-ZIP III and suppress their transcription activities (Kim et al., 2008).

Another important pathway for SAM formation is SHOOT MERISTEMLESS (STM) involved pathway. *STM*, which encodes a transcription factor, belongs to

the class I *KNOX* (knotted1-like homeobox) gene family. *STM* and the *WUS* play in independent pathways but cooperate together in maintenance of SAM. STM prevents stem cells differentiation while WUS keeps activity of stem cells. Three other *KNOX* genes are expressed at the shoot apex in *Arabidopsis*, the *KNOTTED1-LIKE IN ARABIDOPSIS THALIANA* or *BREVIPEDICELLUS* (*KNAT1*/*BP*), *KNAT2* and *KNAT6*. They function similar as the *STM*, prevent cells within shoot apex differentiation into leaf (Byrne ME et al., 2002).

KNOX transcription factors were suggested to function in suppressing gibberellins (GA) and stimulating cytokinins (CK) accumulation in the SAM, which result in maintaining division and preventing differentiation. KNOKs repress GA by inhibiting expression of GA20 oxidase, which is a key enzyme in GA biosynthesis, and concurrently promoting expression of GA2 oxidase, which is an enzyme confining active form in leaf primordia through converting GA into inactive forms (Sakamoto T et al., 2001). KNOXs were also reported to directly activate genes, which encodes isopentenyl transferases (IPTs), important enzymes of CK synthesis. In the *stm* mutant, overexpression of IPTs or application of CK can restore defective meristem (Jasinski et al., 2005).

1.2 Flowering and flower determinacy

1.2.2 Transition of vegetative to reproductive development

Balance between initiation of floral meristem (FM) and keeping shoot meristem activity is controlled by several floral-specific regulated genes, which work on

transition of vegetative to reproductive development. *AP1* and *CAULIFLOWER* (*CAL*), which encode transcription factors, are essential for the inflorescence to floral transition. In double mutant of *AP1* and *CAL*, the primordia fail to develop into floral meristem but continue to produce new inflorescence organs. Overexpression of the *AP1* leads to growth of floral organs instead in inflorescences (Mandel and Yanofsky, 1995). To control the balance between the SAM and the FM, AP1 and CAL are expressed once the floral meristem initiated from inflorescence. The *LEAFY* (*LFY*), which encodes a transcription regulator, participates in inflorescence to floral meristem transition by activation of the *AP1* (Mandel and Yanofsky, 1995). Mutation of the *LFY* causes failure of conversion from inflorescence to floral meristem. To maintain the floral specificity, the expression of *AP1*, *CAL* and *LFY* should be confined in floral primordia. Their expressions are suppressed by *TERMINAL FLOWER* (*TFL*), which depresses floral development. In the *tfl* mutant, expression of *AP1* and *LFY* are elevated and result in turning the whole inflorescence meristem into flower. The AP1 and LFY in turn prevent expression of *TFL* (Bradley et al., 1997). Expressions of *AP1* and *LFY* are also activated by *FLOWER TIMING* (*FT*) gene. It is expressed in leaves, whose encoding proteins or RNA are transported to apex and provide floral signals (Sablowski, 2007).

1.2.2 Floral meristem

During plant development, SAM becomes inflorescence meristem (IM) after

floral transition and its lateral meristem develops into FM. Stem cells in FM are proliferated from IM. FM should be regulated to maintain specificity of floral organs. Thus, development of FM is controlled by many signaling pathways, which have overlapped controlling genes with the SAM. FM development can be perceived as processes of initiation, emergence, and identity. The final step for FM is also critical, activities of FM should be terminated when full set of floral organs have been formed.

1.2.3 ABC model in FM identity

In the *Arabidopsis*, FM identity is under controlled by complex genetic networks, which are described as the ABC model. In this model, A function requires *AP1* and *AP2*, B function requires *AP3* and *PISTILLATA* (*PI*), and *AGAMOUS* (*AG*) belongs to C function gene (Ma and dePamphilis, 2000). All the ABC genes, expect the *AP2*, belong to the MADS-box gene family. Recently, the E function genes are also introduced into ABC model, which include *SEPALLATA1*, *SEPALLATA2*, *SEPALLATA3* and *AGL3*, which were renamed as *SEPALLATA4* (*SEP1*/*2*/*3*/*4*). The ABC model controls FM identity as following: A function genes cooperating with E function genes control the sepal growth. A function genes working with B and E function genes regulate petals formation. B function, C function and E function together control formation of stamens. C function plus E function lead to carpels formation (Ma and dePamphilis, 2000).

Some genes also control FM identity by regulating ABC modeling genes. The

LFY, for instance, besides its function in initiation of FM, is considered to be one of the most important meristem identity genes. The lateral meristem of the *lfy* mutant hardly develops into normal flowers due to developed structures only consisting of sepals and carpels. The *LFY* is epistatic to B function gene, *PI*. It interacts with *AG* in early floral whorl and is also epistatic to *AG* in later whorls (Huala and Sussex, 1992). *LFY* was also considered to interact with the *UNSUAL FLORAL ORGANS* (*UFO*) and *ASK* to control expression of B function genes, *PI* and *AP3* (Zhao et al., 2001).

The C function gene AG takes responsibility of floral meristem initiation at early floral development stage. Expression of *AG* in flowers also determines plant producing carpels and stamens instead of sepals and petals. It is under controlled by several positive and negative regulating genes. *LFY*, the important B function controlling gene, is also a direct positive regulator of *AG* (Parcy et al., 1998). The *WUS* was also considered as an activator of *AG* expression during early floral development stage. In turn, expression of *WUS* is also terminated by AG at stages 4-6 to maintain floral organ specificity. According to previous study, same as *LFY*, *WUS* can bind to cis regulatory region of the *AG* (Lenhard et al., 2001; Lohmann et al., 2001).

Expression of *AG* is repressed by A function gene, *AP2*. Disruption of *AP2* causes extended expression of *AG* and results in formation of carpels and stamens at outer whorl. *AP2* directly represses *AG* transcription in outer whorl by binding to the large *AG* intron (Bomblies et al., 1999). In addition, expression of *AG* is

also negatively controlled by three genes, *LEUNIG* (*LUG*), *SEUSS* (*SEU*), and *BELLRINGER* (*BLR*), whose mutations were observed in enhanced *ap2* mutation. The *lug* mutation causes weak *ap2-l* like phenotypes. The *seu* mutation enhances features of *ap2-1* and shows ectopic expression of *AG*. Mutation of *BLR* causes the formation of carpels replacing of sepals in flowers at late stage of floral development (Conner and Liu, 2000; Franks et al., 2002; Bao et al., 2004).

1.2.4 Termination of floral meristem

After full set of floral organs are initiated, activity of FM should be terminated under control of several signaling pathways to maintain floral organ specificity. In both SAM and FM, *WUS* plays a key role in maintain stem cells by promoting their activities (Mayer et al., 1998). Besides of WUS, AG also plays a significant role in floral meristem determinacy. In the *ag* mutants, activity of the floral meristem lasts longer period than normal. It results in many more floral organs than the wild type plants (Bowman et al., 1989). Thus, *WUS* and *AG* are considered as a positive and a negative regulator of stem cells, respectively. It was known that *WUS* activates expression of *AG* first at stage 3, and *AG* subsequently represses expression of *WUS* at stage 6 (Ming and Ma, 2009). Another gene *KNUCKLES* (*KNU*) was reported to be transcriptional regulated by AG. AG directly binds to the *KNU* promoter region and its binding activates transcription of *KNU*. At stage 6, *KNU* is expressed in a region surrounding WUS expressed OC in the FM. Thus, the *KNU* is considered to inhibit *WUS* expression (Sun et al.,

2009). Recently, *AG* was reported to suppress *WUS* expression by directly binding to the *WUS* and recruiting PcG, Polycomb Group proteins, to *WUS* before stage 6 (Liu et al., 2011). Besides of *AG* and *KNU*, some other genes also play roles in floral determinacy. *SUPERMAN* (*SUP*), for instance, is also involved in termination of *WUS* expression. Besides, genetic studies indicate that *SUP* has independent pathways of *AG* in controlling of the FM (Bowman et al., 1992).

1.3 Male and Female gametogenesis

1.3.1 Stamen development and male gametogenesis

Cells from FM will form four whorls, which develop into four different floral organs from surface to interior: sepals, petals, stamens, and carpels. At the first whorl of opening flowers, sepals are first arisen. At the alternate position of sepals in the second whorl, petals are formed. Six stamens are produced at the third whorl. They are the male reproductive system and are responsible for producing male gametes. The inner whorl consists of gynoecium, fused by two carpels, which provides a place for female gametes formation.

In flower plants, development of male reproductive organs involves initiation and formation of stamens. Each stamen consists of an anther, the chamber for gametogenesis, and a filament, for supporting anther. The filament contains an epidermis and a vascular bundle. The flower and anther development is divided into 14 stages, according to morphological landmarks (Sanders et al., 1999). Floral development begins with the floral meristem, which grow from flower

primordia into sepal primordia at stage 3. At stage 5, four lobes-like chambers are formed and attached to the vascular bundle. Each chamber contains of four protective layers, epidermis, endothecium, middle layer and tapetum layer. Microspore mother cells inside of chambers are surrounded by the four layers. At stage 5, anther morphogenesis is complete. The landmarks for stage 6 are differentiation and division of cells.

At stage 6, each microspore mother cell undergoes one meiotic division and produces a tetrad with four haploid microspores. This is the beginning of male gametogenesis. The microspores dissociate from the outer maternal layers of anthers. This process results in a locule inside of the tapetum layer. The meiotic division completes at stage 7. At stage 8, an enzyme, named as callase, is secreted by tapetum layer. Under activity of this enzyme, each haploid microspore in tetrad separates from tetrad and becomes free microspore. Then, each free microspore increases in size and a huge vacuole is formed inside. Then, the nucleus of each microspore migrates to peripheral area of the cell wall. During stages 9 to 12, uni-nucleate microspores undergo an asymmetric mitotic division, named as Pollen Mitosis I (PMI). This process results in forming bi-cellular microspores, containing a larger cell, the vegetative cell, and a smaller cell, germ cell. The small germ cell is combined within the cytoplasm of vegetative and forms into cell-within-a-cell structure. The asymmetric division is considered to be critical for normal differentiation of germ cell. After PMI, the vegetative cell exits the cell cycle at G1 with dispersed nuclear chromatin. It continues providing nutrition for

further development of germ cell and will give rise to pollen tube once pollinated. The germ cell containing a condensed nuclear chromatin continually undergoes one more mitosis, Pollen Mitosis II (PMII), resulting in two sperm cells. The sperm cells continue cell cycle till G2 and undergo karyogamy (Borg et al., 2009). During stages 11 to 12, the tapetal cells degenerate. At stage 13, dehiscence of anthers occurs and pollen grains are ready to release from stamens. Then, cells in anthers shrink in the following stages (Ma, 2005).

1.3.2 Genes involved in male gametophyte development

Genetic controls of male gametogenesis have been extensively investigated. A large number of genes have been found to participate in male gametogenesis. They play important roles in controlling microsporogenesis and regulating microspore development, asymmetric mitotic division and germline development.

During male gametogenesis, microsporocytes undergo meiosis and develop into tetrad haploid microspores. Preparation of meiosis includes cohesion of sister chromatids from S phase to anaphase II. Genetic controls in this process are also critical for male gametogenesis to proceed. The *DETERMINATE INFERTILE1* (*DIF1*) plays an important role in sister chromatids cohesion in both male and female meiosis. The *dif1* mutation displays multiple meiotic defects and results in sterility (Bhatt et al., 1999).

During meiosis, synapsis of homologous chromosomes is also an essential step, which is controlled by several known genes, such as the *ASYNAPTIC1* (*ASY1*).

The *asy1* mutant shows defective in synapsis at Prophase I and results in defective fertility in both male and female (Sanchez-Moran et al., 2008). Another essential step of meiosis is chromosome segregation, the *ask1* mutation impairs separation of homologous chromosome in anaphase I and segregation of sister chromatids in anaphase II. This mutation also shows male sterility (Liu and Qu, 2008).

When microspores complete meiosis stage, they continue to enter mitotic divisions. The asymmetry division of PMI is essential for formation of male gametophytes. There are some genes showing influences on this progress. Mutation of the *SIDECAR POLLEN* (*SCP*) undergoes a symmetric division following by an asymmetric division, which results in only one fertile daughter cell with only one additional vegetative cell (Chen and McCormick, 1996). Both the *gemini pollen1* (*gem1*) and the *gemini pollen2* (*gem2*) mutants were reported to have effects on gametophytic cytokinesis in PMI. In mature pollen of the *gem1* mutant, only bi-cellular pollen grains are formed (Twell et al., 2002). The *gem2* mutant has no effect on karyokinesis at PMI, it participates in reposition of cell plant as well as disruption of cytokinesis. The mutant results in symmetric divisions and bi-cellular pollen grains (Park et al., 2004).

After PMI, the vegetative cell stops development while the germ cell undergoes a second mitosis, the PMII. Several mutants were reported showing abnormality at PMII. The *cdka1* mutant shows failed division of germ cell and delayed DNA synthesis. Its pollen grains result in a single germ cell, however, with fertility (Nowack et al., 2006). Another gene, the *F-box-Like 17* (*FBL17*), is temporally

expressed after PMI in male gametophyte and targets KPR6 and KRP7, the inhibitors of CDK, which then undergo degradation as ubiquitination substrate. This mutant shows similar features as the *cdka1* mutant (Kim et al., 2008). One other mutant, the *duo pollen (duo)*, also produces pollen with single germ cell. Microspores in the *duo* plants undergo normally asymmetric division at PMI. However, the germ cell blocks at PMII and fails to undergo cell division (Rotman et al., 2005).

1.3.3 Formation of gynoecia and female gametogenesis

In the *Arabidopsis*, a mature female reproductive organ, gynoecium, consists of a stigma, a style and an ovary containing ovules. The stigma is composed of elongated epidermis cells, which take responsibilities of adhering mature pollen grains and inducing pollen germination. It is the beginning of transmitting tract, which facilitates fertilization of ovules. The style is a short cylinder connecting stigma and ovary. The ovary is formed of two carpels, whose margins are connected by replums, and is divided into two chambers. Four rows of ovules in each gynoecium are formed and are protected inside of carpels.

Each ovule development starts from a primordium initiated at the margin of the replum. When an ovule primordium elongates, the nucellus is formed. The hypodermal cell locating at the apex of nucellus undergoes differentiation and becomes an archesporial cell. The archesporial cell then enters meiotic development and differentiates into a megasporocyte. At the same time, epidermal

cells locating at two sides of nucellus divide parallelly and become two primordia, which will be the inner and outer integuments. A megasporocyte then undergoes meiosis and produces four haploid megaspores, among which three megaspores undergo programmed cell death and a functional one remains. The remained functional megaspore grows in size and undergoes the 1st mitotic nuclear division to form a two-nucleate embryo sac. The two nuclei then move to the opposite sides from each other. This movement results in formation of a central vacuole. Then, these two daughter nuclei undergo a karyokinesis and the megaspore results in a four-nucleate embryo sac. The central vacuole continues to increase in size and the four nuclei undergo a third karyokinesis. After the third karyokinesis, an eight nucleated embryo sac is formed. Among the eight nuclei, two polar nuclei migrate to micropolar cytoplasm of embryo sac and combine to form a diploid central nucleus. During formation of central nucleus, cell walls are formed concurrently. The eight cells are classified into three antipodal cells, one diploid central cell, two synergids, and an egg. The antipodal cells are quickly degenerated after central nucleus formed. The central cell, synergids and egg are formed into a functional unit to facilitate fertilization, including attracting pollen tube, cooperating with tube to help sperms release, and completing double fertilization (Yang et al., 2010).

1.3.4 Genes involved in ovule development

Germline cells are first initiated from archesporial cells, which are differentiated

from the ovule primordia locating at hypodermal L2 cell layers. The essential transition of archesporial cells from somatic fate to germline fate is controlled by the *SPOROCYTELESS* (*SPL*)/*NOZZLE* (*NZZ*) gene. Mutation of *SPL* displays defected germline cells in both male and female organs (Schiefthaler et al., 1999).

After transition into germline fate, archesporial cells differentiate into the megasporocytes. Each of them then undergoes meiosis and produces four haploid megaspores. Three megaspores undergo program cell death and the functional one is survived. Many genes were reported to be required at first karykinesis. We will describe one as an example. AGL23 belongs to Type I MADS-box family and its mutation blocks development of ovule at one nucleate embryo sac. In addition, the expression patterns of AGL23 are found in functional megaspores and in embryo sacs, which indicate that *AGL23* is essential for first meiotic division of female megagametogenesis (Colombo et al., 2008). Even many mutations were observed to cause a defect at the first mitosis, little knowledge was known about its genetic mechanism.

Many genes are involved in mitotic divisions have been identified, which provide rich information about cell division progression in regulating female gametogenesis. A group of genes encoding proteins belonging to ubiquitin/ proteasome system are involved in controlling cell cycle progression of mitotic divisions. The anaphase-promoting complex/ cyclosome (APC/C), an E3 ligase, participates in mitosis process. As reported in previous studies, mutation of *NOMEGA*, which encodes of APC6/CDC16, or mutation of *APC2*, that cooperates

with APC11 and APC8/CDC23, will lead to arresting mitotic division at two-nucleate cell stage (Capron et al., 2003; Kwee and Sundaresan, 2003). Another study indicated that the Regulatory Particle Triple A ATPase (RPT) of 26S proteasome are involved in female mitotic division. The *rpt5a-4rpt5b-1* double mutant shows arrested development at the first or the second mitotic divisions (Liu et al., 2008; Gallois et al., 2009). The results suggest that the ubiquitin/proteasome system is involved in controlling cell cycle during female gametogenesis.

Many genes encoding transcription factors and other regulatory proteins have been reported in controlling cell cycle progress. For instance, *RETINO BLASTOMA RELATED* (*RBR*) gene is an important negative regulator of G1/S transition by repressing the transcription factor, E2F. The *rbr* mutant shows blocked mitosis and abnormal nuclear proliferation. This mutant results in forming of extra nuclei. Mutation of *RBR* also causes premature of ovule at two or four nucleate stages. Moreover, the *rbr1-1/+* plants or the *rbr1-1/+* plants pollinated by WT can produce abnormal embryos. This indicates that complement of three nuclei division is essential for normal embryo formation (Ebel et al., 2004).

After formation of four nucleated embryo sac, two pairs of nuclei are divided from each other by a central vacuole and move to their opposite sides. The nuclei then undergo migration, precise position, and cellularization. The central cell, synergids and egg are formed into a functional unit. Some genes are specifically

expressed in gamete unit and are essential for it. For egg cells, *GAMETE EXPRESSED3* (*GEX3*) is expressed in the egg cells specifically. Defect of *GEX3* impairs pollen tube guidance in female micropyle during fertilization (Alandete-Saez et al., 2008).

For synergid cells, they mainly work on recognition and attracting of pollen tubes as well as transportation of sperms. The *MYB98*, which encodes a R2R3-type MYB transcription factor, is particularly expressed in the synergid cells. The *myb98* mutation shows impairing of filiform apparatus formation and results in lost the pollen tube guiding in micropyle (Punwani et al., 2007). Synergids also play roles in reception of pollen tube. *FERONIA* (*FER*)/*SRN* is expressed in synergids and functions in recognition between pollen tube and synergid. *FER* encodes a LRR-RLK, which particularly locates at the plasma membrane of synergid cells. And in the *fer*/*srn* ovules, pollen tubes enter synergids and overgrowth inside of embryo sac. The death of synergid cells was reported to relate with the *GFA2* gene, which encodes a mitochondrion located DnaJ domain–containing protein. Interestingly, this gene encoded protein localizes in mitochondrial matrix and its mutation shows persist of synergids after pollination (Christensen, 2002; Yu et al., 2005; Escobar-Restrepo et al., 2007; Punwani et al., 2007).

Several reports also investigated genes, which control central cells. The *DIANA* (*DIA*) gene, which encodes a transcription factor belonging to the MADS-box family, participates in controlling development of central cell. The mutation of

DIA fails in fusion of polar cells into a central cell and results in an abnormal central nucleus, which cannot be fertilized after pollination. Besides, the central cell specific marker cannot be detected inside of ovule. AGL80 was reported to work with DIA, they form a heterodimer. Defect of *AGL80* fails in maturation of central cell due to failure of polar nuclei maturation (Favaro et al., 2003; Portereiko et al., 2006). Genes expressed in the central cell may be also involved in fertilization. The *GLAUCE* (*GIC*) will be described as an example. Mutation of it shows no effects on embryo sac as well as the gamete cells, but its ovule fails to be fertilized (Ngo et al., 2007).

1.3.5 Mutations affecting both male and female gametogenesis

Many genes are essential for both male and female gametophytes. Before formation of megaspores, transition from the somatic fate into the germline fate is required for both male and female gamete mother cells. The *SPL* / *NZZ* gene is considered to control transition of germline fate. In the *spl*/*nzz* plants, archesporial cells in L2 of anther and ovary primordia fail to develop into germline cells and lead to failure in both male and female sporocytes formation (Yang et al., 1999).

Genes, that are essential for meiotic and mitotic divisions, usually affect both male and female gametogenesis. For meiosis, sister chromatid cohesion is a pre-condition. The mutation of *SYN1*/*DIF1* causes abnormal condensation and pairing of chromosome, which leads to severed chromosome segregation. Ovules in the *syn*/*dif1* plants hardly form embryo sac inside. This mutation shows

defective in both male and female fertility (Bhatt et al., 1999). Another important gene involved in sister chromatid cohesion during meiosis is the *SWITCH1*/*DYAD*. Mutation of *swi1*/*dyad* causes a mitotic division instead of meiosis in female, which results in no embryo sac formation in ovules. In male meiosis of the *swi1*/*dyad*, chromatids are unevenly separated at first and second meiotic divisions, which result in extra nuclei production. The extra nuclei is degenerated later (Liu and Qu, 2008).

Many genes were reported to take responsibilities in chromosome pairing, synapsis and recombination during meiosis. Disruption of these genes also impairs both male and female meiosis. An example is SPO11, whose homologs in yeast functions in double-strand break formation. The *spo11–1* mutant produces polyads in male gametophytes due to disruption of homologous chromosome pairing, recombination and formation of bivalent. Besides, there is no formation of the embryo sac in ovules (Grelon et al., 2001).

Another gene, *GEM2,* is considered to be critical in gametophytic cytokinesis. The *gem2* mutant displays defective in gametophytic cytokinesis of PMI. Besides this feature, it also shows asymmetric mitotic division in embryo sac, which leads to five nuclei at the one side, the micropylar pole, and three at the opposite site, the chalazal pole (Twell et al., 2002; Park et al., 2004).

1.4 Embryogenesis

1.4.1 Introduction to embryogenesis

In the life cycle of plants, there is an alternation between haploid to diploid generations. Following male and female gametogenesis, the egg and polar nuclei in ovule are fertilized by sperm cells and produce a zygote that undergoes embryogenesis and a triploid cell that forms endosperm. Embryogenesis is divided into three phases. First part, zygotes develop into embryonic organs with specificity of shoots and roots. Second stage is maturation of embryos and final phase is termination of development and desiccation.

After combination of two gametes, zygote is polarized according to the relative position of nucleus and vacuole, and it gets elongated concurrently. Then, zygote undergoes lateral division and becomes two daughter cells. The smaller one is apical cell and the larger one is basal cell. The basal cell then develops into suspensor and hypophysis. The apical cell undergoes first cell division in vertical and suspensor undergoes a transverse division. The two apical cells form into embryo proper, which undergoes another longitudinal division and becomes a four-celled embryo proper. Meanwhile, the suspensor also undergoes another transverse division. The octant stage embryo is formed after a transverse division of quadrant embryo proper. The octant embryo proper is then divided by a cleavage, which is parallel to the surface, and becomes a sixteen-celled embryo, a dermatogen embryo. Among the sixteen cells, the cells in protoderm undergo one

division, which is perpendicular to the surface, and the interior cells undergo another longitudinal division. The divisions result in the early globular stage. At the same time, the top cell of the suspensor undergoes a transverse division to produce the hypophysis. During the next stage, mid-globular stage, the hypophysis continues a longitudinal division; interior cells in embryo proper undergo both longitudinal and transverse divisions, protodermal cells also undergo divisions. After multiple cell divisions, the buttresses appear and the apical pole is broader, which are the markers of transition stage. After that stage, the heart stage comes, the cotyledonary lobes grow symmetrically and increase in size. At linear cotyledon stage, cotyledon structure is completed, which includes apical domain, cotyledon, shoot apex, and upper axis. At the same time, the central domain consists of axis and basal domains contains root apex. During the embryo development, the cells inside of embryo store nutrition for growth. Suspensor consisting of 6 to 11 cells functions as a conduit for nutrition sending from endosperm to maternal tissues and provides growth factors for embryogenesis.

During the phase of maturation, embryonic cells accumulate macromolecules including proteins, lipids, and carbohydrates. Those become the nutrition sources of seedling. After maturation, embryos stop growth and undergo desiccation. Finally, seeds enter a metabolic quiescence period and remain dormant until meet an appropriate condition for germination (West and Harada, 1993).

1.4.2 Genes involved in embryogenesis

Previous studies have reported variety of genes involved in the progress of embryogenesis. The WRKY DNA-BINDING PROTEIN 2 (WRKY2), a transcription factor, is required in zygote polarization by inducing expression of *WOX8* and *WOX9*. In the *wrky2* mutant, the nucleus and vacuole of zygote is mis-localized while the polarity of egg cell is not affected. This also indicates that polarity regulation of egg and zygote is independent (Ueda et al., 2011).

Before division, zygote undergoes elongation. The GDP/GTP exchange factor for small G proteins of the ARF class (ARF-GEF), which is also called GN, was reported to participate in zygote elongation. The *gn* mutant impairs in both elongation and asymmetric division of zygote (Busch et al., 1996).

Then, the zygote divides into an apical and a basal cells, which requires cooperation of several pathways. The apical-basal axis establishment requires the transcription factors, WOX8, WOX9, and WOX2, which are also involved in polarization of zygotes. *WOX8* and *WOX9* are expressed in the basal cell and *WOX2* is expressed in the apical cell (Lau et al., 2012). It was reported that *WRKY3* was co-expressed with *WOX8* and regulates expression of *WOX8* and *WOX9*. The *wox8wox9* double mutant and the *wox9* mutant both show defective in embryos. Embryo defect also exists in the *wox2* mutant (Ueda et al., 2011). Auxin signaling pathways also regulate establishment of the apical-basal axis. Apical division of zygote is directly affected by directional auxin transport. The mutation

of *PIN-FORMED 7* (*PIN7*) encoding an auxin efflux regulator results in a transverse division instead of a longitudinal one in apical cells of embryos. The *MONOPTEROS* (*MP*), which encodes an auxin response factor, and *BODENLOS* (*BDL*), which encodes an inhibitor of AUX/IAA, both are expressed in apical cells and required in specificity of apical cell division. The similar phenotype as the *pin7* mutant were observed in *mp* and *bdl* as well as the *mp bdl* double matant (Hamann T et al., 1999; Friml J et al., 2003).

The original formation of radial-patterned embryo begins from octant stage (Schlereth et al., 2010). Cell divisions are controlled by *WOX* regulated pathways and auxin signaling pathways. The mutations related to WOX pathways, such *wox2, wox8wox2, wox2mp,* and *wox1wox2wox3*, cannot form completed protoderm (Breuninger et al., 2008). Some genes locating at inner cells are also required for radial pattern formation. For example, SHR, a transcriptional factor of GRAS, is initially expressed in provasculature and then transported to the neighboring cell layers. It then induces SCR, another transcriptional factor GRAS, and is expressed in inner cells. Both SHR and SCR function in periclinal cell divisions (Nakajima K et al., 2001).

Shape of embryo proper is regulated by several hormone signaling pathways, such as auxin and brassinosteroid (BR). In the apical domain, in order to form separated cotyledonary primordia, outgrowth of center structure is suppressed by *CUP-SHAPED COTYLEDON1* (*CUC1*), *CUC2*, and *CUC3*. Double mutations of either two cause fused cotyledons and loss of shoot meristem. The *CUC* genes

encode homolog proteins of petunia NO APICAL MERISTEM (NAM). The *nam* mutant shows the similar phenotype with the *cuc* mutant in defected separation of cotyledons. The spatial expression patterns of CUC1 and CUC2 are under control by MP and PIN7, which are involved in auxin signaling pathways (Aida M et al., 2002). Some other genes were also suggested to be essential in cell division of central cells. For example, the *FACKEL* (*FK*) gene plays an important roles in forming sterols for proper embryo development. Its mutation shows failure of central cell elongation and asymmetrically divisions resulting in abnormality in apical and basal domains as well as formation of multiple shoot meristems and cotyledons. FK is considered to be required in BR signaling pathway and functions as BR receptor. (Schrick K et al., 2002).

1.5 Program cell death

1.5.1 Program cell death in plants

Program cell death (PCD) is an essential process during development of organisms and a proper response to stress environments. PCD is considered to be a self-controlled process causing cell death of unwanted cells. In plants, PCD shares common morphological and biochemical features with animal cell apoptosis, which include shrinkage of the cytoplasm, condensation and aggregation of the chromatin, fragmentation of the nuclear DNA into oligonucleosomal ladders (Gadjev et al., 2008).

The vacuoles and the chloroplasts are plant-specific organelles, which function

in controlling of plant cell death through signaling pathways. Vacuoles are considered to mediate cellular lysis through producing a variety of metabolites, which function in defense or in recycling of cellular components. Vacuoles in plants are also involved in autophagy, a mechanism for breaking down damaged and harmful particles or degeneration of cellular components for nutrients recycle. Autophagic cell death begins with an increased size of vacuole, then target organelles swallowed by the vacuole and organelles undergo degradation. Finally, continuous lysis of the vacuole results in cell death (Hatsugai et al., 2006).

Chloroplasts are important sources of signals to induce PCD. In chloroplast, reactive oxygen species (ROS), such as hydrogen peroxide and superoxide, are produced by photosynthetic electron transport chains under abiotic and biotic stress conditions. Chloroplast-derived molecules including hydrogen peroxide, singlet oxygen function in inducing PCD through transducing signaling between chloroplast and nucleus under stress conditions (Gadjev et al., 2008).

Mitochondria were considered to be prominent players in animal cell death (Balk et al., 1999). In plant, mitochondria may cooperate with chloroplast signals in PCD. Mitochondria and released cytochrome c were reported to participate in different types of plant PCD, such as formation of tracheary elements, self-incompatibility and heat-shock induced cell death (Yu et al., 2002).

1.5.2 Program cell death in biological progresses

PCD is a fundamental process for plant development. It is involved in many

biological processes starting as early as female megagametogenesis and embryogenesis. PCD also occurs in degeneration of tapetum layers in anthers, germinating seeds, formation of aerenchyma, differentiation of tracheary elements, remodeling of leaf shape, and leaf senescence (Gadjev et al., 2008).

During female gametogenesis, megasporocytes undergo two meiotic divisions and form four megaspores. Three of the megaspores undergo PCD and one functional megaspore is survival. After three times of karyokinesis, the megaspore become an eight-nucleate embryo sac. Among the eight cells, three antipodal cells in one side of ovules undergo cell death immediately before fertilization. The polar cells function in providing signals to attract and guide the pollen tube and undergo cell death after pollination.

After fertilization, zygote is formed and undergoes transverse division into apical and basal cells. Apical cells will develop into embryo propers while basal cells will become suspensors. A channel is formed in the suspensor to send growth factors into the embryo proper for a short time and is then degenerated by PCD (Bozhkov et al., 2005).

During anther development, PCD is also a critical process to keep male fertility. At stages 11-12, tapetum layers undergo degeneration by cell death manner. This process facilitates anther dehiscence and allows pollen exposure.

Development of tracheary elements in the xylem of vascular plants is another well-studied model system of plant PCD. The differentiation of mesophyll into xylem is caused by nucleases and proteases produced in the vacuole and with

reticulation of the cell walls. During the process of autolysis, the swelled vacuole is destructed, nuclear DNA and organelles are fragmented. ROS play important roles in the autolysis during tracheary elements differentiation (Lam, 2005).

1.5.3 Reactive oxygen species regulate program cell death

Reactive oxygen species (ROS) were considered to be key modulators of PCD. ROS are produced in organelles including chloroplasts, mitochondria, peroxisomes, and cytosol.

In previous studies, ROS induced cells death was observed in many development processes as well as in stress responses. MAPKs are involved in the H_2O_2 signals pathway. Among the MARKs, the MAPK kinase kinase MEKK1, which is regulated by different stresses and hydrogen peroxide, directly interacts with WRKY53, which is a transcription factor regulating induced PCD in senescence (Miao et al., 2007). Nucleotide diphosphate kinases are also involved in ROS signaling networks. *NUCLEOTIDE DIPHOSPHATE KINASE2* (*NDK2*) is also induced by hydrogen peroxide. Overexpression of the *NDK2* reduces hydrogen peroxide levels and elevates tolerance of oxidative stress (Moon et al., 2003) . The ROS networks function in ROS induced cell death through transmitting signals to ROS-specific transcription factors. Such as the zinc finger transcription factors, LSD1 and LOL1, function in negative and positive regulators of ROS-induced cell death, respectively (Epple et al., 2003).

1.6 Summary and perspectives in this study

Plant development is an intelligent and complicated system. It involves precise regulation of complex pathways and networks to ensure proper development and reproduction.

Flower formation, gametogenesis, and embryogenesis are the main processes for plant sexual reproduction. . Over last decades, many genes involved in these processes have been identified and characterized. However, a lot more genes and pathways remained to be identified and studied.

This project focused on analysis of the roles of two Arabidopsis genes in the reproductive processes. One of them, AtANA1, was initially identified as a redox-sensitive protein, and the other one, AtPUB4, is an E3 ubiquitin ligase and was previously reported to function in tapetal cell growth and degeneration. It has been shown through this study that ANA1 functions in both gametogenesis and embryogenesis. PUB4 was found to be an important player in controlling floral meristem determinacy. This study contributes to understanding of additional components involved in these important reproductive developmental processes.

Chapter Two- Materials and Methods

2.1 Plant materials

Arabidopsis thaliana ecotype Columbia (Col-0) was used as wild type in this study. The single mutants, *Atana1-1/+, Atana1-2/+, qrt* and *pub4*, were obtained from Arabidopsis Biological Resource Center. The single mutant of $ag10^{lers}$, $ag10^{col}$, and *WUSpro::GUS* transgenic $ag10^{lers}$ lines were provided by Xuemei Chen (Liu et al., 2011).

The line of *Atana1-1/+ qrt/qrt* was obtained by crossing *Atana1-1/+*with *qrt/qrt*, and *Atana1-1/+ qrt/qrt* was selected from the F2 progenies. The *xlg1-2xlg2xlg3* triple mutant was obtained from F2 progenies by crossing between *xlg1-2xlg2* and *xlg3*.The lines of $ag10pu4^{col}$ *and* $ag10pub4^{lers}$ were obtained from F2 generation of progeny plants, which were obtained by crossing *pub4* with $ag10^{col}$ and $ag10^{lers}$.

2.2 Plant growth condition

Arabidopsis plants planted on soil were grown in a greenhouse at Hong Kong Baptist University.

Arabidopsis seeds were first sterilized with 70% ethanol for 10 min, and then by 100% ethanol containing of 0.2% triton X for 10 min. After ethanol removal and air drying, the sterilized seeds were then plated on Murashige and Skoog (MS) medium (Murashige and Skoog, 1962) with 1% sucrose, vernalized at 4 °C for 2 days and then cultured in a growth camber under a 16h light and 8 h dark

photoperiod.

For ectopic floral organs cultured on plate, external silique was sterilized with 20% bleach containing 0.1% (v/v) Triton X-100 for 30 min, and subsequently washed with double-distilled water for at least three times. The sterilized tissue was plated in MS medium and cultured in growth camber with 16h light and 8h dark repeat cycle.

2.3 PCR analysis and T-insertion lines

To confirm the mutation lines, PCR was performed with genomic DNA of *Atana1-1/+, Atana1-2/+,* and *pub4, ag10*^{ler}*, ag10*^{col} using the gene-specific oligonucleotides. T-DNA flanking sequence of the ana1 allele in *Atana1-1/+*was amplified by using a T-DNA left border primer LBD and ANA1-1-RP. T-DNA flanking sequence of the ana1 allele in *Atana1-2/+*was amplified by using a T-DNA left border primer LBD and ANA1-2-RP. T-DNA flanking sequence of the pub4 allele was amplified by using a T-DNA left border primer LB and PUB4-RP. For *ag10* genotyping, PCR was performed on genomic DNA using primers AG10scrf 5'and AG10scrf 3', and the PCR products were digested by ScrFI (The primers will be provided in Table.2.3)

2.4 Constructing vectors

To construct *pBar:ANA1pro:GUS*, a 1019bp ANA1 promoter was amplified from genomic DNA by primers *ANApro 5'* and *ANApro 3'* and cloned into pMD18-T.

The fragment containing *EcoRI* and *SpeI* was sub-cloned into binary vector pBar:GUS.

To construct *pBar:35S:ANA1:eYFP*, A 1022bp ANA1 coding region was amplified from Arabidopsis cDNA preparation by primers *ANA-eYFP5'* and *ANA-eYFP3'* and first cloned into pMD18-T vector. This fragment containing *KpnI* and *XbaI* was cut and sub-cloned into binary vector pBAR:35S:eYFP.

To construct *CHF3-ANA1Comp*, a 4090 fragment containing ANA1 genomic DNA, 1494bp upstream and 1018bp downstream sequences was amplified from WT plants (Col-0) by primers *ANA Comp5'* and *ANA Comp3'*. This fragment containing *kpnI* and *PstI* was sub-cloned into pCHF3 for complementation.

To construct *pET-41aPUB4,* a 2493bp fragment was amplified from cDNA by primers *PUB4cdna5'* and *PUB4cdnd3'* and cloned to pMD18-T. Then this PUB4 fragment containing *NcoI* and *SalI* was cut and sub-cloned into pET-41a vector.

2.5 Bacterial strains and plasmids

The bacterial strains used in this study are listed in Table 2.1. The plasmids constructed in this study are listed in Table 2.2

Table 2.1 Bacterial strain used

Bacterial strains	Description
A. tumefaciens GV3101	$Gent^r$, rif^r used for plant transformation
E. coli DH5	Used for transformation and propagation of recombinant plasmids

E.coli JM110	Used for transformation and prevent methylation on Xbal restriction enzyme cutting site
E.coli BL21	Used for inducing protein expression

Table 2.2 Plasmids and constructed vectors

Plasmids	Description	Source
pMD18-T	A vector containing single 3'-T overhangs at the insertion site for the cloning of A-tailed PCR products and containing of multiple restriction enzyme sites	Takara
pBar: GUS	A binary vector with multiple cloning sites flanked by a promoter-less GUS gene and containing of kanamycin resistance for selection.	
pBar:35S:eYFP	A binary vector with multiple cloning sites containing a CaMV 35S promoter with eYFP gene and kanamycin resistance.	
pET-41a	A vector containing of multiple cloning site fused with GST tag for protein expression	Novagen

2.6 Oligonucleotide primers

Table2.3 Oligonucleotide primers used

Primers	Sequence	Description
M13F	CGC CAG GGT TTT CCC AGT CAC GAC	DNA sequencing
M13R	TCA CAC AGG AAA CAG CTA TGA C	DNA sequencing
T7	CTA GTT ATT GCT CAG CGG TG	DNA sequencing
GUS 5’	CTGGTATCAGCGCGA AGTCT	DNA sequencing
GUS 3’	AGTCGAGCATCTCTTC AGCG	DNA sequencing
ANA1-1LP	TAGATGACGACGTGG ATCTTATTGA	Left genomic primer of T-DNA, works with ANA1-1RP to test WT allele
ANA1-1RP	TGGTTAGGTTATACTT CGGTTTGG	Right genomic primer of T-DNA, works with LBD to test T-DNA insertion alleles.
ANA1-2LP	AGCACTTTTACACGTC CTGTCTATC	Left genomic primer of T-DNA, works with ANA1-1RP to test WT alleles
ANA1-2RP	TGTGGGCAACCCAAA CAATAT	Right genomic primer of T-DNA, works with LBD to test T-DNA insertion alleles
LBD	TAGCATCTGAATTTCA TAACCAATCTCGATAC AC	Left border primer of the T-DNA insertion, for SAIL lines
ANA pro 5’	AGGTACCTGTAGCAC TCACTTATAGATGGTT GAA	For cloning of 1019 bp *ANA1* promoter fragments to construct *pBAR:ANApro::GUS*, the *KpnI* site is underlined
ANA pro 3’	ATCTAGAAATGGAGA AATCTATGTAAAACCT CG	For cloning of 1019 bp *ANA*1 promoter fragments to construct *pBAR:ANApro::GUS*, *XbaI* site is underlined
ANA Comp5’	AGGTACCCGGGACGG TTTGTTGGAAGAG	Cloning a 4090 fragment containing ANA1 genomic DNA, 1494bp upstream and 1018bp downstream. The *KpnI* site is underlined
ANA Comp3’	ACTGCAGGTTGAAGA ATGGCGGGAAGCA	Cloning a 4090 fragment containing ANA1 genomic DNA, 1494bp

		upstream and 1018bp downstream. *PstI* site is underlined
ANA-eYFP 5’	AGGTACCTCTTATTCCTCTTCAAAGGCAAAC	Amplifying ANA1 from CDS to construct pBAR:35S: ANA :eYFP, *KpnI* site is underlined
ANA-eYFP 3’	ACTGCAGCAAATTATACGAAAGGGCACAAA	Amplifying ANA1 of CDS to construct pBAR:35S: ANA:eYFP,. *Xbal* site is underlined
RT-ANA 5’	CAAAGGAGAGTGACATTGGCTG	Real-time quantitative PCR for ANA1
RT-ANA 3’	CTTCCAAGAAGGTTTCTTTGCC	Real-time quantitative PCR for ANA1
PUB4-LP	CAAGACTCGACAGACCCTGAC	Left genomic primer of T-DNA, works with PUB4-RP to test WT allele
PUB4-RP	AATTCTCCTTGGCTTCAGAGC	Right genomic primer of T-DNA, works with LB to test T-DNA insertion alleles
PUB4-pet 5’	CCCATGGTGGAAATGGAAGTTC	Cloning of PUB4 cDNA to construct expression vector pET41a-PUB4, *NcoII* site is underlined
PUB4-pet 3’	GTCGACTCAGCCACGCCCAGCGTT	Cloning of PUB4 cDNA to construct expression vector pET41a-PUB4, *ScaI* site is underlined
XLG3-LP	CTTCTTCTTCTTGTTCTGTGTTCGTCTTC	Left genomic primer of T-DNA, works with XLG3-RP to test WT allele
XLG3-RP	GCTCTAAGCACACAGTTTCCACAATACTT	Right genomic primer of T-DNA, works with LB to test T-DNA insertion alleles
AG10scrf 5’	CCCAAAGAGCTCAGGAACCTG	Forward primer of 100bp AG sequencing, which containing of site mutagenesis on *ScrfI* restriction enzyme digestion site
AG10scrf 3’	TAGCAACAAGGCATATAGAT	Reverse primer of 100bp AG sequencing, which containing of site mutagenesis on *ScrfI* restriction enzyme digestion site
LB	ATTTTGCCGATTTCGGAAC	Left border primer of the T-DNA insertion, for Salk lines
RT AG 5’	GAGGAACAATCCGAGTATAAGTCTAATG	Real-time quantitative PCR for AG
RT AG3’	CGCGGATGAGTAATGGTGATT	Real-time quantitative PCR for AG

RT AP1 5’	CTCTTGTTGTCTTCTC CCATAAGGG	Real-time quantitative PCR for AP1
RT AP1 3’	GGACTCAGGTGCAAT AAGCTGTC	Real-time quantitative PCR for AP1
RT CLV3 5’	CTGCTTCTTGTTCCTT CATGATGC	Real-time quantitative PCR for CLV3
RT CLV3 3’	CATTTGCTCCAACCCA TTCAC	Real-time quantitative PCR for CLV3
RT KNU 5’	CACCGTCTTACCTTCA TTTCGTAG	Real-time quantitative PCR for KNU
RT KNU 3’	GTTTTGGTGACCGCC GAGAG	Real-time quantitative PCR for KNU
RT WUS 5’	CGACGGAGCAAATCA AAATCC	Real-time quantitative PCR for WUS
RT WUS 3’	CTGACGCTCACGAGC CTTATG	Real-time quantitative PCR for WUS
RT STM 5’	CTCTGTCAAGGCCAA GATCATGG	Real-time quantitative PCR for STM
RT STM3’	GACATCCTGTTGGTCC CATAGATG	Real-time quantitative PCR for STM
ACTIN2 5’	GGTAACATTGTGCTCA GTGGTGG	Real-time quantitative PCR for ACTIN2
ACTIN2 3’	AACGACCTTAATCTTC ATGCTGC	Real-time quantitative PCR for ACTIN2

2.7 Polymerase chain reaction (PCR), restriction enzyme digestion on plasmid, product purification and ligation

The PCR amplification of gene fragments was performed following the PCR protocol of Phusion® High-Fidelity DNA Polymerase (NEB). The PCR analysis of plant genomic DNA was performed following the PCR protocol of *Taq* DNA Polymerase (Takara).

Corresponding restriction enzymes were applied to plasmids for digestion. The mixtures were set up according to the protocols of corresponding restriction endonucleases (NEB) and incubated at 37 °C for 2 to 4 hr. The digested fragments

were then separated in 1% agarose gel by electrophoresis. The target fragments were excised and purified by using zymoclean gel DNA recovery kit (Zymo research).

The ligation mixture containing of insert gene fragment and vector at appropriate proportion as well as T4 ligase incubated at room temperature for 1hr according to procedure of T4 DNA ligase (NEB).

2.8 Preparation of *Agrobacterium tumefaciens* competent cells and *Arabidopsis* transformation

A newly-streaked colony of *GV3101* from a double-yeast-tryptone medium (DYT) agar plate supplemented with gentamycin and rifampicin (Invitrogen) was inoculated in 2 ml DYT medium and incubated for 24 hr at 28 °C with 250rmp shaking. The culture was then sub-cultured in 50 ml of LB medium in 250 ml flask for overnight shaking at 28°C with 200 rpm till OD600 value reached 0.6. The culture was chilled on ice for 20min and collected by centrifugation at 6000g for 10min at 4°C. The competent cells were aliquoted (200 µl) into 1.5 ml Eppendorf tubes and immediately frozen in liquid nitrogen.

Constructed plasmid DNA (0.1-1 µg) was added to competent cells, mixed well and incubated on ice for 5 min. The cells were frozen in liquid nitrogen for about 1-5 min and immediately thawed at 37 °C for about 5 min. 800ul DYT was added to the transformed cells, which were then incubated at 28 °C with gentle shaking (200 rpm) for 2hr. The cells were pelleted by centrifugation at 6000 rpm for 1 min

at room temperature and were re-suspended with 100ul DYT. The suspended cells were subsequently spread on DYT agar plates supplemented with the appropriate antibiotic(s). The plates were incubated at 28 °C for 2 days.

A newly-grown colony of transformed agrobacterium on DYT agar plate was picked up and inoculated in 2ml DYT medium with appropriate antibiotics for 24-30 hr at 28 °C with 250 rmp shaking. Then, the cultured medium was sub-cultured in 200ml DYT medium in 500ml flask for overnight at 28°C with 250 rmp shaking till the OD600 value reaching 1.0-2.0. At this time, the cells were collected by centrifuge at 8000rmp for 8 min. The pellet was re-suspended by 100ml infiltration medium containing of 1xMS, 5% sucrose and 0.02% silwet at PH 5.7. The floral dip was performed in this re-suspended medium for 10 min and the transformed plants were covered immediately. The next day, the plants were uncovered and normally cultured.

2.9 Transgenic lines selection and analysis

The transgenic plants were *Atana1-1Comp*, *Atana1-2Comp*, *AtANA1pro:GUS*, *35S: eYFP* and *35S: AtANA1: eYFP*, *WUSpro::GUS pub4*, *WUSpro::GUS ag10pub4*, *DR5::GUS pub4* and *pub4Comp*.

The complementation lines were obtained by transforming *CHF3-ANA1Comp* vector into *Atana1-1/+* and *Atana1-2/+* heterozygous plants. In the T2 generation, several homozygous lines of *CHF3-ANA1Comp* transgenic *Atana1-1* and *Atana1-2* were identified, which were named as *Atana1-1comp* and

Atana1-2comp, respectively. The *Atana1-1Comp* and *Atana1-1Comp* lines were then selected by collecting seeds from T2 plants independently and treated with BASTA. The plants, whose progenies were all resistant to BASTA, were *Atana1-1Comp* and *Atana1-2Comp*.

The *AtANA1 pro::GUS* transgenic lines were obtained by transforming *AtANA1 pro::GUS* into WT *Arabidopsis*. The transgenic lines were selected by BASTA resistance feature through the T1 progenies.

The stable transgenic plants of *35S: eYFP* were obtained by transforming *pBar:35S::eYFP* from agrobacterium into *Arabidopsis* through floral dip. For the stable *35S::ANA1:eYFP* transgenic Arabidopsis, *pBAR:35S::ANA1:eYFP* vector was transformed by *Agrobacterium*-mediated transformation into *Arabidopsis*. The transgenic lines were selected by BASTA resistance feature through the T1 progenies.

WUSpro:GUS pub4 and *WUSpro:GUS ag10pub4* were obtained at F2 generation of progeny plants after crossing between *pub4* and *WUSpro:GUS* transgenic *ag10*. The *DR5::GUS* transgenic *pub4* plants were obtained at F2 generation of progeny plants after crossing between *pub4* and *DR5:GUS*.

2.10 Extraction and purification of genomic DNA

Genomic DNA from *Arabidopsis* rosette leaves were first ground into fine power in liquid nitrogen. Cetyltrimethyl ammonium bromide (CTAB) buffer (400 µl) containing 2% (w/v) CTAB, 1.4 M NaCl, 20 mM EDTA (pH 8.0), 0.1M Tris-HCl

(pH8.0) and 0.2% (v/v) β-mercaptoethanol were added and the suspension was placed at 65 °C for 10 min. After the samples were cooled down, 400ul chloroform was added to each tube containing of tissue mixture. The components in suspension were separated by centrifugation at 8,000rpm for 5min. After collecting the supernatant, the genomic DNA mixture was purified by adding same volume of chloroform. After separation of centrifugation of 8,000rmp for 5min, the supernatant was transferred into new tube and the equal volume of isopropanol was added to precipitate genomic DNA. After incubation for 1hr, the genomic DNA was precipitated by centrifugation at 8,000 rpm for 10 min. The resulting pellet was washed with 70% (v/v) ethanol. After air drying, genomic DNA was re-suspended in 50ul distilled water and stored at -20°C for future use.

2.11 Extraction of plant total RNA and cDNA synthesis

Plant total RNA was extracted by using the Aligent plant RNA isolation Mini Kit (Aligent technologies) following the manufacturer's instruction. The target Arabidopsis tissues were first collected from plants and frozen in liquid nitrogen immediately for further use. The frozen tissues were grinded into fine powder with mortar in liquid nitrogen. The homogenized plant tissues then treated following the protocol of Aligent plant RNA isolation mini kit.

When the purified RNA was obtained, RNA samples were then treated with gDNA Erase to remove contained genomic DNA (PrimeScript™ RT reagent Kit with gDNA Eraser (Perfect Real Time), Takara). The treated RNA samples then

underwent reverse transcription into cDNA by PrimeScript™ RT reagent Kit following the manufacturer's protocol (TAKARA). The extracted RNA samples were stored at -80 ^{o}C and synthesized cDNA was stored at -20^{o}C.

2.12 Real-time quantitative PCR analysis

The mixture of real-time quantitative PCR was set up following the protocol of the SYBR Premix Ex Taq II. cDNA template as well as the specific primers were added in a volume of 25ul per reaction (SYBR Premix Ex Taq II, Takara). The transcript changes were analyzed by at least three independent replicates. The primers utilized in real-time quantitative PCR analysis were shown in Table 2.3. The transcriptional changes were detected and collected by Stratagene Mx3000P

2.13 β-Glucuronidase (GUS) histochemical assays

β-Glucuronidase (GUS) histochemical staining assays were performed by applying the standard X-Gluc staining solution (50mM sodium phosphate buffer pH7.0, 10mM EDTA-disodium salt, 0.2% (v/v) Triton X-100, 20 µl 20 mg/ml 5 bromo-4-chloro-3-indolyl β-D glucuronide [X-Gluc] stock solution, 2mM potassium ferricyanide and 2mM potassium ferrocyanide) to the plant tissues. The samples in staining solution were treated with vacuum for 1 hour for better infiltration and kept at 37 ^{o}C overnight in the dark. Samples then were washed by 70% ethanol for several times and observed under an Olympus SZX18 microscope.

2.14 Wax sectioning

Target tissues were separated from plants and fixed in FAA solution (50% Ethanol, 5% Formaldehyde, 10% acetic acid, and 35% ddH20). The samples were infiltrated by vacuum in FAA for 4 hr. Samples then underwent dehydration in ethanol series (50%, 60%, 70%, 85%, 95% and 100%) for 30min-1hr each. Samples were washed by 100% ethanol two more times repeating for completely dehydration. The paraplast infusion of embedding tissues was performed by replacing ethanol into xylene. The dehydration samples were incubated in solution containing of 25% xylene and 75% ethanol for 1hr, then replaced by 50% xylene and 50% ethanol for the next hour. After incubation in 75% xylene and 25% ethanol solution for 1hr, the sample was incubated in 100% xylene and washed by 100% xylene for two more times. 1/4 bottle volumed paraffin chips (Leica) were added to the bottle containing of tissue sample and 100% xylene and incubated overnight. The next day, more paraffin chips were added in till filled half volume of bottle and incubated for several hours. The xylene-paraplast mixture was replaced by melted paraplast solution at 65°C and replacement of paraplast solution was performed at least 6 times. (6-8 hr between each replacement) The tissues were embedded in paraffin block and cooled down in 4°C for overnight. The embedded tissues were sectioned by microtome with 8um to 10um thick. The paraffin ribbons was mounted on wet slides and air dried. The sectioned tissues were stained with 0.5% toluidine blue, then de-waxed by xylene for 2-3 times.

After the xylene was volatized, the slides were observed through a light microscope (ZEISS).

2.15 Terminal Deoxynucleotidyl Transferase dUTP Nick End Labelling (TUNEL) assay

Whole inflorescences were sampled and treated following the protocol of wax sectioning. The sectioned tissues were deparaffinized by immersing in xylene for 5min. The samples were then washed by immersing the slides in 100% ethanol for 5mins. Then, the samples were rehydrated by graded ethanol washes (100%, 95%, 85%, 70% and 50%) for 3 minutes each at room temperature. After rehydration, samples were washed by 0.85% NaCl and then washed in PBS for 5 min. Samples were then permeated by a 20ug/ml proteinase K solution for 10mins. After washing by PBS for 5min, samples were fixed in 4% (v/v) paraformaldehyde in PBS for 5min. This followed by another PBS wash for 5 min. Nick-end labeling of fragmented DNA was performed following Dead End Fluorometric TUNEL system (Promega) according to the manufacturer's instructions. The samples on slides were treated with 100µl of Equilibration Buffer for 10min and stained by 50 ul rTdT incubation buffer in dark at 37^{o}C for 1hr. Then, samples were stained in 1 µg/mL of propidium iodide (PI) and mounted with clear nail polish. Samples were then observed under a fluorescence scanning confocal microscope (Leica TCS SP5 II) using excitation at 488 nm and emission at 509 nm to view the yellow/green fluorescence of rTdT and a 538/617-nm excitation/emission

spectrum to view the red fluorescence of PI.

2.16 Light microscope observation and confocal microscope observation

For pollen viability staining, anthers/pollen grains were stained with Alexander staining solution (1% malachite green, 1% orange G, 10% (v/v) ethanol, 25% glycerol, 0.05% acid fuchsia, and 4% acetic acid) for several minutes and observed though light microscope (ZEISS) or dissection microscope (Olympus SZX18).

For whole mount ovules and embryos observation, inflorescences or siliques were collected from plants and fixed with 9:1 ethanol/acetic acid solution overnight. After washing in 90% ethanol and then 70% ethanol, samples were cleared with choral hydrate: glycerol: water (8:1:2 w:v:v) solution. The tissues were dissected and observed through a Nikon Eclipse 800 wide-field epifluoresence microscope with a differential interference contrast (DIC) optic.

For 3,3'-Diaminobenzidine (DAB) staining, samples were collected from plants and treated with DAB solution containing of 1 mg/ml DAB. Samples in DAB solution were gently infiltrated by vacuum for several hours and incubated overnight. The next day, DAB solution were removed and replaced by bleaching solution (ethanol: acetic acid: glycerol 3:1:1). When the color of samples were washed out, samples were observed through the Olympus SZX18 dissection microscope.

For 4',6-diamidino-2-phenylindole (DAPI) staining of pollen grains,

inflorescences were collected and dissected from plants. Then, each anther containing pollen grains was applied with DAPI staining solution (0.1 M sodium phosphate (pH 7), 1 mM EDTA, 0.1% Triton X-100, 0.4 μg/ml DAPI; high grade, Sigma) and incubated for several minutes. The slides with pollen grains were observed through confocal microscope using a 340–380 nm excitation filter and a 450–480 emission filter (Leica TCS SP5 II).

For the determination of subcellular localization, the seeds of *35S*::*eYFP* and *35S::ANA1:eYFP* transgenic plants were collected and seeded on MS plates. The roots of seedlings were observed through Leica TCS SP5II confocal microscope under 500-530 nm wavelength.

2.17 Protein expression, purification and in vitro ubiquitination assay

Constructed expression vector, *pET-41PUB4*, was transformed into *BL21* competent cells and grew on agar plate. One colony was picked up for inoculated in 2ml LB and cultured overnight. 0.5ml culture was sub-cultured in 50ml LB at 250ml flask till the OD_{600} value reaching 0.4. At this time, the IPTG was added to reach the final concentration at 1mm IPTG and cultured for 4 hr. Cells containing of expressed proteins were harvested by centrifugation at 5,000g for 10min. And the proteins in cells were extracted by treatment with B-PER Reagent following the manufacturer's protocol (B-PER® Bacterial Protein Extraction Reagent, thermo scientific). Then, the GST-tag fused PUB4 was purified by Pierce® GST Spin Purification Kit following their manufacturer's procedures (thermo

scientific). The PUB4 was eluted from spin column and can be stored in 4^{o}C for one week.

The E3 ligase activity was tested by incubation with PUB4 (500ng), as E3 ligase, with 0.6ul 0.1M ATP, 1ug Flag-ubiquitin, 60ng human E1 (UBE1), 300ng human E2 (Ubc E2), and 3ul 10x ligase assay buffer (500 mM Tris-HCl, pH 7.4,50 mM MgCl2, 20 mM NaF, 6 mM dithiothreitol (DTT), 100 nM okadaic acid.) to the final volume of 30ul each reaction. A known E3 ligase (His-MurF1, human recombinant) was treated in another reaction as positive control. The mixture was incubated in 37^{o}C for 1hr and stopped by boiling with 30ul 2x DTT-SDS. The reaction mixture was separated by SDS-polyacrylamide gel electrophoresis (SDS-PAGE) on a 10% gel and then transferred to a nitrocellulose filter. The ubiquitination results were performed by standard immunoblotting analysis with anti-Flag M2 antibody.

Chapter Three-AtANA1 is Required for Gametogenesis and Embryogenesis

3.1 Introduction

Programmed cell death (PCD) is a self-controlled process leading to induced death of unwanted or damaged cells in eukaryotes. In animal cells, apoptosis has been well studied (Lawen, 2003). In plants, PCD shares common morphological and biochemical features with animal cell apoptosis, which include shrinkage of the cytoplasm and fragmentation of the nuclear DNA into oligonucleosomal ladders (Wang et al., 1996). In last two decades, biochemical and genetic regulations on PCD have been investigated extensively in plants. One of important modulators of PCD is reactive oxygen species (ROS) (Gadjev et al., 2008).

ROS, such as hydrogen peroxide (H_2O_2) and superoxide anion (O_2.-), act as second messengers to activate signaling cascades responding to environmental cues (Averyanov, 2009). ROS signal transduction networks have been identified in controlling plant PCD, including protein kinases and transcription factors (Gadjev et al., 2008). The oxidative modification of redox-sensitive proteins by ROS is an important mechanism to modulate oxidative stress responses as well as plant developmental processes (Ghezzi, 2005; Poole and Nelson, 2008).

In previous study, we have identified 84 redox sensitive proteins in the *Arabidopsis* cells through redox proteomics approaches, which are based on differential labeling of oxidized and reduced thiols by 5-iodoacetamidofluorescein (IAF), a fluorescent derivative of thiol-reactive iodoacetamide (IAM) (Ghezzi and

Bonetto, 2003; Wang et al., 2012). One of those redox sensitive proteins is AtANAMORSIN1 (abbreviated as ANA1). BLAST search revealed full sequence of *AtANA1* shares 32% identity with the Anamorsin in humans and 68% identity with Dre2 in yeast. That indicates AtANA1 is a member of the Anamorsin / cytokine-induced apoptosis inhibitor 1(CIAPIN1) family. CIAPIN1 was initially considered as a cytokine-induced anti-apoptotic protein in mice. Knock out Anamorsin in mice leaded fetal death at the late gestation due to apoptosis of hematopoietic cells in liver (Shibayama et al., 2004). In yeast, DRE2 was reported to be one part of an electron transfer chain at the early biogenesis stage of cytosolic Fe-S proteins. DRE2 was then shown to form a stable complex with TAH18 (Vernis et al., 2009). The Tah18-Dre2 cluster was considered to be essential for yeast viability (Soler et al., 2011).

ANA1 was found to become more oxidized in *Arabidopsis* cells in response to treatments of H2O2 and other redox-perturbing chemicals, such as Flg22 or SA (Wang et al., 2012). In the *Arabidopsis*, AtANA1/ AtDRE2 (AtDRE2 was named in (Bernard et al., 2013)) was reported to form a complex with AtTAH18. This complex also functions as an iron-sulfur (Fe-S) cluster in electron transfer chain. Loss-of-function mutation of the *AtDRE2/AtANA1* showed embryos lethality in the *Arabidopsis* (Bernard et al., 2013).

Gametogenesis and embryogenesis are essential productive processes for flowering plants. During male gametogenesis, microsporocytes undergo one meiotic division and produce a tetrad of four haploid microspores. Microspores

undergo PMI and then PMII to give rise to one vegetative germ cell and twin germ cells (Borg et al., 2009). During female gametophytes development, megasporocytes undergo a meiotic division and produce four haploid megaspores. Three of them undergo program cell death and one functional megaspore remains, which becomes embryo sac. The functional megaspores undergo three karyokinesis, and give rise to eight-nucleate embryo sacs (Yang et al., 2010).

As the beginning of embryogenesis, a zygote undergoes lateral division to produce an apical cell and a basal cell, which will continue to undergo cell divisions and become an embryo proper and a suspensor, respectively. Apical cells continue to undergo transverse and longitudinal divisions and become quadrant, octant, dermatogen, globular, heart and linear cotyledon stage. Meanwhile, basal cells undergo several transverse divisions and become suspensor. Finally, embryo results in an embryonic axis with shoot poles, root poles and cotyledons (Harada, 1993). Many cellular processes in the reproductive development require involvement of signaling pathways to regulate cell divisions, differentiations and the morphogenesis. Mutations of key components involved in both embryogenesis and gametogenesis lead to embryonic lethality and/or sterility, making it difficult to recover such mutants for detailed characterization or for identification of important genes in regulating both processes by forward genetic approaches.

In this study, we carried out functional characterizations of the *AtANA1* gene. *AtANA1* was found to be required for embryogenesis and its mutation is embryogenic lethal. In addition, the ana1 mutation also affects gametogenesis. It

was found that the ana1 mutation caused programmed cell death of embryonic tissues and gametophytes.

3.2 Results

3.2.1 Loss-of-function mutation of *Atana1* leads to embryonic lethality

To study function of the *AtANA1* (At5g18400) gene, two T-DNA insertion mutagenized lines, SAIL_808_G09 and SAIL_1222_B12, were obtained from the Arabidopsis Biological Resource Center. Their T-DNA insertion sites were confirmed by PCR analysis and by sequencing T-DNA- flanking genomic fragments (Figure 3.1a). The mutation lines, SAIL_808_G09 and SAIL_1222_B12, with different insertion sites, are named *Atana1-1* and *Atana1-2,* respectively, in this report. The *AtANA1* encodes a 272 amino acid protein. The region between amino acids 182 and 263 has high sequence similarity to CIAPIN domains from other members of the Anamorsin /CIAPIN1 family. *ana1-1* and *ana1-2* were derived from transformation by The T-DNA insertion vector pDAP101, which carries a BASTA resistant gene in its T-DNA. We identified the *Atana1-1/+* heterozygous plants by BASTA selection and PCR analysis. However, when the heterozygous plants were self-pollinated, we only obtained homozygous wild type (WT) plants and the heterozygous plants. Failure of identifying homozygous progenies of the *Atana1* allele indicates that loss-of-function mutation of *AtANA1* may cause embryonic lethality.

Developing carpels and siliques from heterozygous plants were further examined to reveal whether they exhibit embryonic lethality. As shown in Figure 3.1c and 3.1d, a majority of ovules in the heterozygous plants undergo fertilization while a few ovules fail to be fertilized. In siliques of the *Atana1-1/+*

self-pollinated plants, development of some embryos aborted at early stages. As shown in Figure 3.1e, the aborted embryos in *Atana1-1/+* and in *Atana1-2/+* self-pollinated plants became brownish and shrunken at early embryo development stages while normal seeds remained green and round.

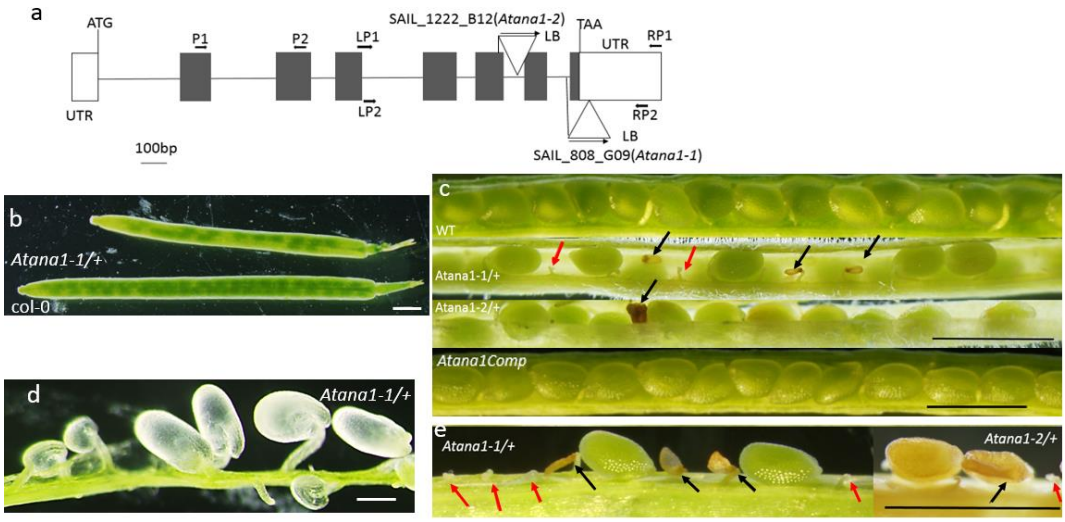

Figure 3.1. The *Atana1* mutation causes embryonic lethality and impairs female gametogenesis

(a) Schematic representation of the *AtANA1* gene and insertion sites of two mutations. Open boxes, filled boxes and lines represent untranslated regions (UTR), exons and introns, respectively.

(b) Comparison of siliques from WT and the self-pollinated *Atana1-1/+* plants.

(c) Siliques of WT, the *Atana1-1/+*, the *Atana1-2/+,* and the *Atana1Comp* plants. The *Atana1-1/+* and the *Atana1-2/+* plants show some aborted embryos (black arrows) and ovules (red arrows).

(d) Opened *Atana1/+* silique 1 day post-pollination showing abnormal ovules.

(e) Portion of an 8 day post-pollination silique from *Atana1-1/+* and a mature silique from *Atana1-2/+*. The black arrows point to aborted seeds. The red arrows point to aborted ovules or unfertilized ovules.

The scale bars in Figure 3.1c, 3.1d, and 3.1f represent 1mm, in Figure 3.1e represents 125um.

3.2.2 *AtANA1* disruption blocks embryogenesis

Siliques of *Atana1-1/+* were dissected and observed through a dissection microscope to count the number of aborted seeds in the self-pollinated progeny. The *ana1* mutation was found not only causing embryonic lethality but also affecting development of both male and female gametophytes (see below). The *Atana1-1/+* self-pollinated siliques contained 15.69% (129/822, 822 is the total number of aborted ovules, aborted embryos, and normal embryos) aborted embryos while WT only showed 1.6% (10/625) aborted embryos (Table3.1). To reveal at what stage the embryogenesis fails to proceed, clear whole-mount embryos at different development stages were observed through a DIC optic. During a normal development process, a zygote undergoes the first cell division to form an apical cell and the basal cell. Apical cell then undergoes continuous vertical and transverse divisions to develop into embryo proper. Embryo proper proceeds through an octant stage, then the globular, heart and torpedo stages. In the *Atana1-1/+* self-pollinated siliques, when majority of embryos were at the octant stage, about one quarter (129/538=23.98%, 538 only contains aborted embryos and normal embryos) of embryos were arrested after the first cell division. Both the cells and the nuclei of both apical cell and the basal cell in mutant embryos were apparently abnormally large but no further cell division occurred beyond this stage (Figure 3.2f-j) while normal embryos continued to grow through the early globular stage (Figure 3.2b), the late globular stage (Figure 3.2c), the transition stage (Figure 3.2d) and the heart stage (Figure 3.2e). During

observation through whole development, few (1.68% =10/597) abnormal seeds from the heterozygous plants were found to be able to develop beyond the first division but were arrested at a late stage (Figure 3.2h). This ratio is similar with the aborted embryo rate in WT, 1.6%. Thus, we believe the delayed situation is due to the environmental factors.

Table 3.1. The rate of aborted seeds and ovules setting in WT and *Atana1-1/+* self-pollinated plants

Genotype	Total number of seeds and ovules	Normal seeds		Aborted seeds		Aborted ovules	
		#	%	#	%	#	%
WT	625	600	96%	10	1.6%	15	2.4%
Atana1-1/+	822	409	49.76%	129	15.6%	284	34.67%

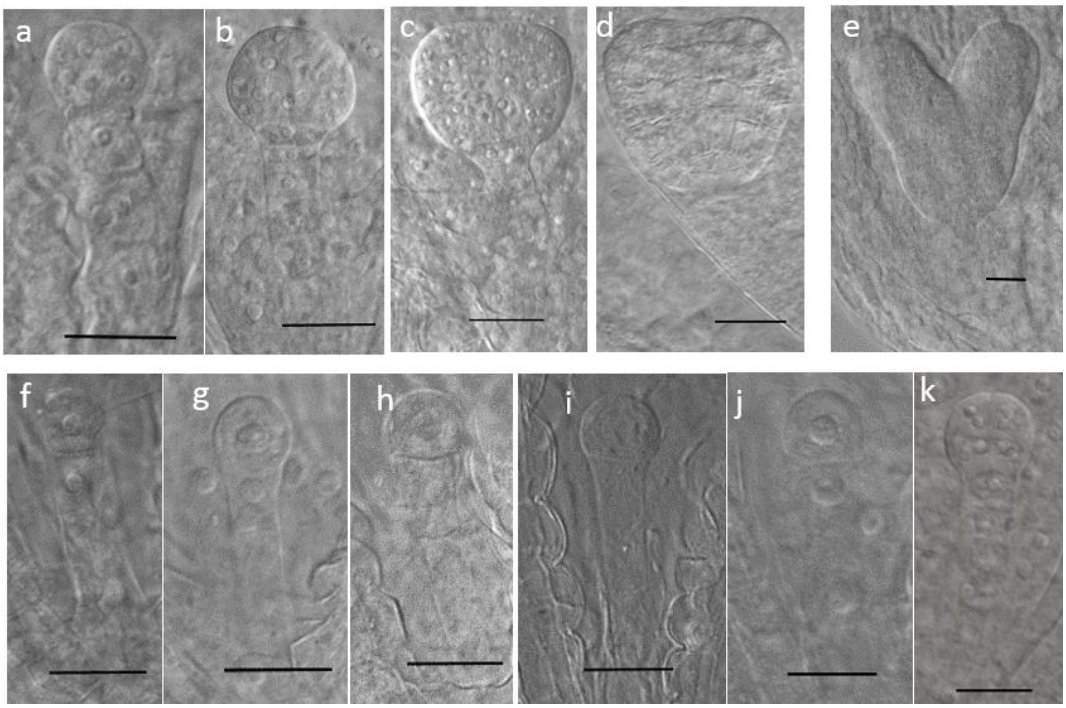

Figure 3.2. The *Atana1-1/+* heterozygous plants show embryogenesis arrest after first division of zygotes

Whole-mount developing seeds are at various stages from the *Atana1-1/+*plants. Embryos in the (a) and (f), (b), (g), and (k), (c) and (h), (d) and (i), (e) and (j), are from the same siliques, respectively.

(a, b, c, d, e) Normal embryos are at the octant (a), early globular (b), late globular (c), transition (d) and heart (e) stage, respectively.

(f, g, h, i, j) Defective embryos arrested after the first division of zygote. The apical and the basal cells and their nuclei were enlarged.

(k) Defective embryos with delayed growth stage comparing to the normal embryos (b) in same silique.

The scale bar in each figure represents 25um

3.2.3 *AtANA1* Disruption causes abortion of some ana1 pollen and also affect neighbouring wild type pollen

If defect of *AtANA1* only causes embryos lethality, the segregation ratio of one *Atana1/+* self-pollinated heterozygous plant is supposed to be 2:1 (heterozygous: WT). However, using BASTA resistance as the marker of the mutant allele, the segregation ratio of progeny from the self-pollinated *Atana1-1/+* plant heterozygous plants were found to be 1.29:1 (72: 56), suggesting that the *ana1* mutation also affects gametogenesis. This notion was supported from the observed aborted ovules in the heterozygous plants. To investigate the effect of the *Atana1* mutation on male gametogenesis, the viability staining of pollen was performed by Alexander staining (Alexander, 1969). The Alexander staining results showed that almost all pollen of WT (98.55%, 825/838) are viability while about 41.7% (418/1003) pollen from the *Atana1-1/+* plants show non-viability (Figure 3.3a). This result indicates that male gametogenesis was impaired by the *Atana1* mutation. Assuming that the heterozygous plants produce 50% of ANA1 pollen and 50% of ana1 pollen, the result suggests that only approximately 8% of the *ana1* pollen grains were viable. The earlier observation showed that approximately 16% of *ana1* ovules were normal. If this is indeed the case, only 1.3% of embryos produced in self-pollinated heterozygous plants are expected to have a homozygous *ana1* genotype. However, the number of aborted embryos was much higher than expected one.

We examined the transmission rates of the ana1 allele through male and female gametophytes by reciprocal crosses with WT plants. The progenies were examined by their resistance to BASTA. The *ana1* transmission rates through male and female gametophytes were found to be 58.4% and 93.02%, respectively (Table 3.2). The female and male transmission rates combined together results in 13.56% homozygous seeds, while the calculated aborted seeds were 15.5%. The embryo lethality rate can also match with theoretical number from male and female transmission rates.

Table 3.2 Transmission rates of the ana1 allele through male and female

Cross (Female by Male)	Progeny phenotype		TE_M (%)	TM_F (%)
	Atana1-1/+	+/+		
+/+ by *Atana1-1/+*	104	178	58.4%	NA
Atana1-1/+ by +/+	80	86	NA	93.02%

(TE_M represents transmission rates though male, TE_F represents transmission rates though female.)

The above results raise a possibility that some of the pollen grains showing negative viability staining could be ANA1 pollen, which became aborted because of close association with aborting ana1 pollen. To address this question, we crossed the *Atana1-1/+* plants with the *quartet (qrt)* mutant to obtain the *Atana1-1/+ qrt/qrt* mutant. In the *qrt* mutant, four microspores (tetrad) derived from the same pollen mother cell remained attachment during the subsequent gametogenesis due to fused outer walls of four meiotic products (Preuss et al., 1994). Thus, under the *qrt/qrt* background, each tetrad produced in the *Atana1-1/+* plants contains two pollen with the mutant *Atana1-1* allele and the

other two carrying the wild type allele. Viability of tetrads from the *qrt/qrt* plants and the *Atana1-1/+ qrt/qrt* plants were determined by Alexander's staining. As shown in Figure 3.3b and 3.3c, almost all pollen grains in the *qrt* plants were viable; however some of tetrads from the *Atana1-1/+ qrt/qrt* contained a single aborted pollen, suggesting that not all ana1 pollen grains underwent abortion. A majority of tetrads had two aborted pollen. Interestingly, some tetrads have three or four aborted pollen grains. The result indicates that aborting ana1 pollen grains caused abortion of some pollen carrying the wild type allele.

DAPI staining of nuclei and morphological observation also showed that some tetrads had three or four aborted pollen grains (Figure 3.3d). In total, 214 of 224 pollen in the tetrads from the qrt/qrt plants were viable. Among 197 pollen grains from the Atana1-1/+ qrt/qrt plants, 77 had four viable pollen, 13 tetrads had three pollen, 36 tetrads had two viable pollen, 26 tetrads had one pollen, and 45 tetrad had no viable pollen (Table 3.3). In total, 43.5% of the pollen from the Atana1-1/+ qrt/qrt mutant was not viable, which is close to the rate of aborted pollen observed in the Atana1-1/+ plants (41.7% 418/1003). The results also suggest that aborting of pollen carrying the WT alleles does not have to be attached through tetrads. Due to the condition of tetrad pollen grains in ana1-1/+, we have reason to believe that wild type female gametes could be also affected by its neighboring mutant female gametes. This could be the reason of high female transmission rate after crossing by WT. The mechanism of unequal transmission rates between male and female will be discussed in later chapter.

Table 3.3. Numbers of tetrads with different numbers of aborted pollen in the *Atana1-1/+ qrt* plants and *qrt* plants

	Four viable pollen	one viable pollen	two viable	Three viable pollen	All aborted	Total tetrad
qrt	214	10	0	0	0	224
Ana1-1/+ qrt/qrt	77	13	36	26	45	197

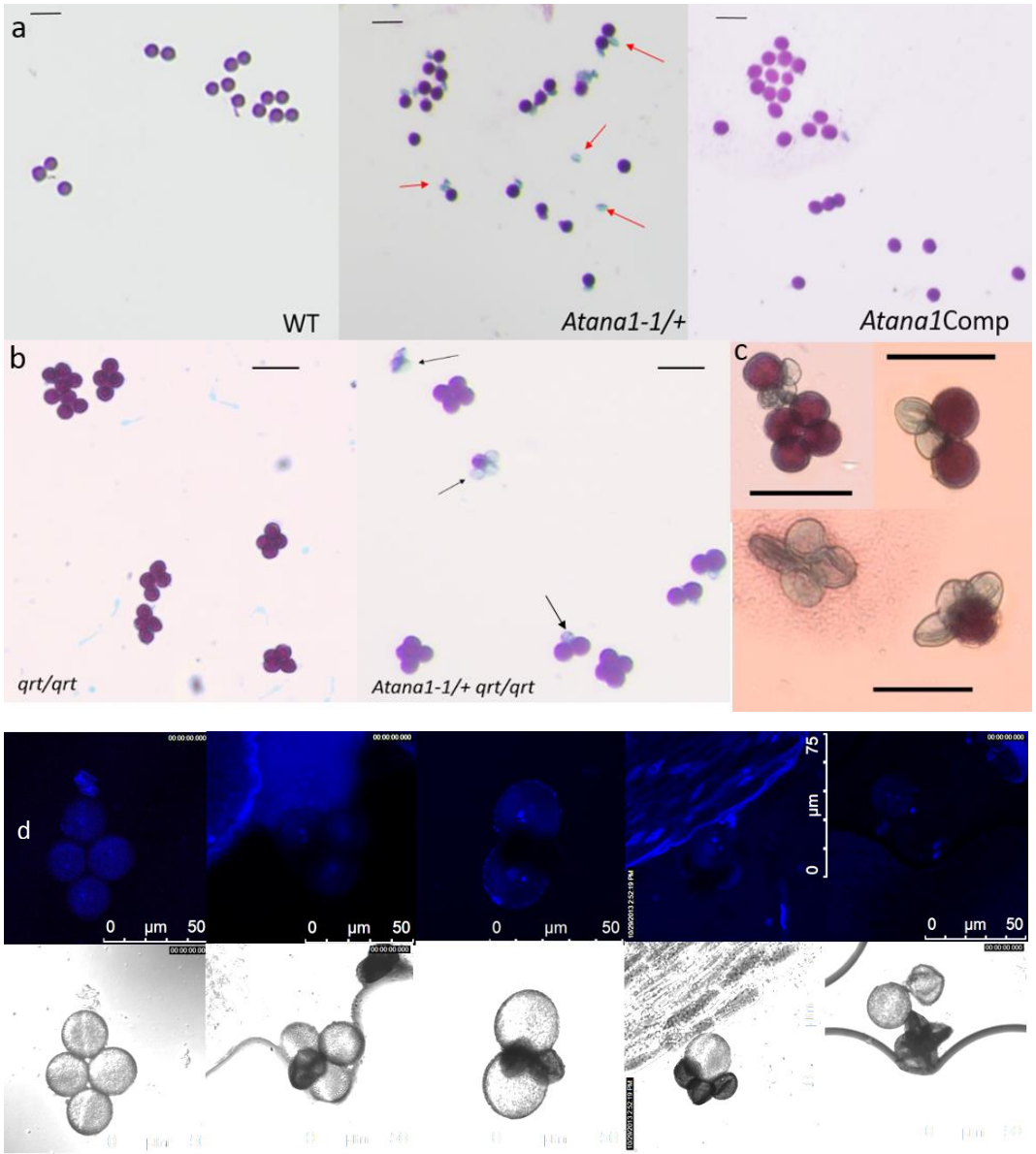

Figure 3.3. *Atana1-1* mutation impairs male gametogenesis

(a) Alexander viability staining results of pollen grains from WT, *Atana1-1/+*, and *Atana1Comp* plants. The pollen grains showing purple color were viable. The red arrows pointing the non-viable pollen grains from the *Atana1-1/+* plant, which cannot be stained by Alexander staining buffer.

(b) Alexander staining results of the *qrt/qrt* mutant and the *Atana1-1/+ qrt/qrt* mutant. The black arrows point to some of non-viable pollen grains.

(c) A close-up view of Alexander stained tetrads show four viable tetrad pollen, three viable tetrad pollen, two viable tetrad pollen, one viable tetrad pollen and non-viable tetrad pollen.

(d) DAPI staining of pollen grains from the *Atana1-1/+ qrt/qrt* plants with corresponding bright field microscope images are shown. Pollen with nuclear stained and reflected fluorescence were viable, whereas the aborted pollen showed no DAPI staining and appeared shrunken in the bright field images.

Scale bars in Figure 3.3a, 3.3b and 3.3c represent 50um. Scale bars in Figure 3.3d are labeled in each figure.

3.2.4 Disruption of *ANA1* causes abortion of male gametophytes before PMI

To determine at what stage the ana1 mutation causes a defect in male gametogenesis, pollen grains at different developmental stages were examined by DAPI staining. Pollen grains from the *Atana1-1* plants under the *qrt* background provided an ideal model for this observation, in which two *Atana1* gametophytes can be compared with two wild type gametophytes from the same tetrad. In *Arabidopsis*, each pollen mother cell undergoes meiosis to form four haploid microspores (a tetrad). Nuclei inside unicellular microspores undergo migration to peripheral position against the cell wall. Then, unicellular microspores undergo an asymmetric division, PMI, to become bi-cellular microspores containing one vegetative cell and one germ cell. Finally, every germ cell undergoes another mitotic division, PMII, to produce twin sperm cells, which is called a tricellular stage.

We did not find an obvious difference between microspores from WT and *Atana1-1/+* at the tetrad stage (Figure 3.4a and 3.4b). At the unicellular stage, two of tetrad pollen from the *Atana1-1/+* plants arrested development and showed condensed nuclei (Figure 3.4c and 3.4d). At the early bi-cellular stage, the asymmetric division produced a diffusely stained vegetative cell and an intensely stained generative cell. Comparing two normal gametophytes, two mutation ones show low DAPI signals (Figure 3.4e and 3.4f). In the tri-cellular stage, when two intense nuclei were stained, the nuclei inside mutation pollens were degraded and their shapes were shrunken (Figure 3.4g and 3.4h). The DAPI staining results indicate that the *Atana1* mutation causes abortion of male gametophytes before

PMI.

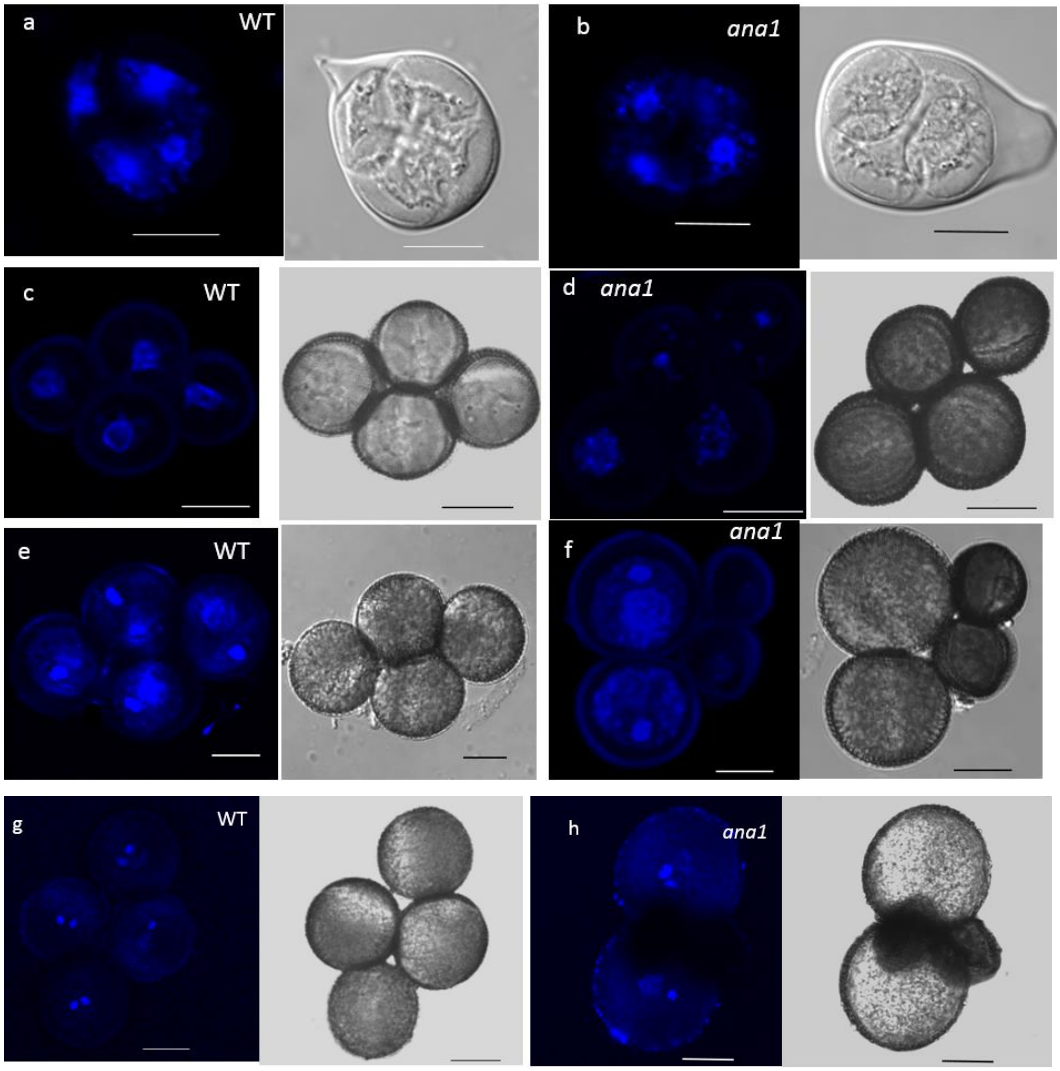

Figure 3.4. DAPI stained nuclei and corresponding bright field images of male gametophytes from the *qrt* and the *Atana1-1/+ qrt/qrt* plants at different stages

(a, c, e, g) Gametophytes at tetrad stage (a), unicellular stage (c), bicellular (e) and tricellular stage (g) from the *qrt* plants, respectively.

(b, d, f, h) Gametophytes at tetrad stage (b), unicellular stage (d), bicellular (e) and tricellular stage (h) from the *Atana1-1/+qrt/qrt* plants, respectively.

Scale bars in all figures represent 10um.

3.2.5 The *Atana1* mutation arrests female gametogenesis during mitosis

Microscopic observation was carried out to reveal the defect in female gametogenesis caused by the *Atana1-1* mutation. First of all, the aborted ovules or unfertilized ovules were counted from young siliques of heterozygous plants (Figure 3.1c). The percentage of aborted or unfertilized ovules from the *Atana1-1*/+ plants was 34.55% (284/822) while that of WT was 2.4% (15/625) (Table 3.1). Assuming that 50% of the ovules produced from the heterozygous plants had the mutant allele, approximate 36% (411-(284– 20)/411 = 35.76%) of the *Atana1-1*/+ ovules from *Atana1-1*/+ plants are functional. However, the result of female transmission rates through reciprocal crosses was 93.02% (80/86) (Table 3.3). The result raises a possibility that aborted some of the aborted ovules could be those carrying the WT allele.

To determine when female gametogenesis fails to proceed in the *Atana1* ovules, clear whole-mount ovules at different developmental stages were observed through a DIC optic. For normal female gametogenesis, a megaspore (Figure 3.5a) undergoes three mitotic divisions without cytokinesis to produce two (Figure 3.5b), four (Figure 3.5d), and eight (Figure 3.5g) nucleate embryo sacs. Ovules from the same pistil were considered to be at the same development stage. The stage at which majority of megagametophytes exhibited was considered as the normal developmental stage in each pistil. In *Atana1-1*/+ pistils, some of megagametophytes were found to arrest at earlier stages. At the one nucleate stage,

we could not find any obvious differences among the developing megagametophytes (Figure 3.5a). At the two nucleate stage (Figure 3.5b), some defective megagametophytes remained at the one nucleate stage (Figure 3.5c). At the four nucleate stage (Figure 3.5d), the defective megagametophytes were found to be at one or two nucleate stage (Figure 3.5e and 3.5f). At the eight nucleate stage (Figure 3.5g), a few (0.83% 1/121) megagametophytes remained at the four nucleate stage (Figure 3.5h), 14.87% (18/121) megagametophytes were arrested at the two nucleate stage (Figure 3.5i), and 23.96% (29/121) were at one nucleate stage (Figure 3.5j) (Table 3.4). In total, 39.69% of the megagametophytes showed abnormality with abortion occurred apparently at different stage.

Table 3.4. The number of arrested megagametophytes at different stages in *ana1-1/+* pistils

	One nucleate	Two nucleate	Four nucleate	Eight nucleate	Total
Counting number	29	18	1	73	121
Percentage	23.97%	14.88%	0.83%	60.33%	#

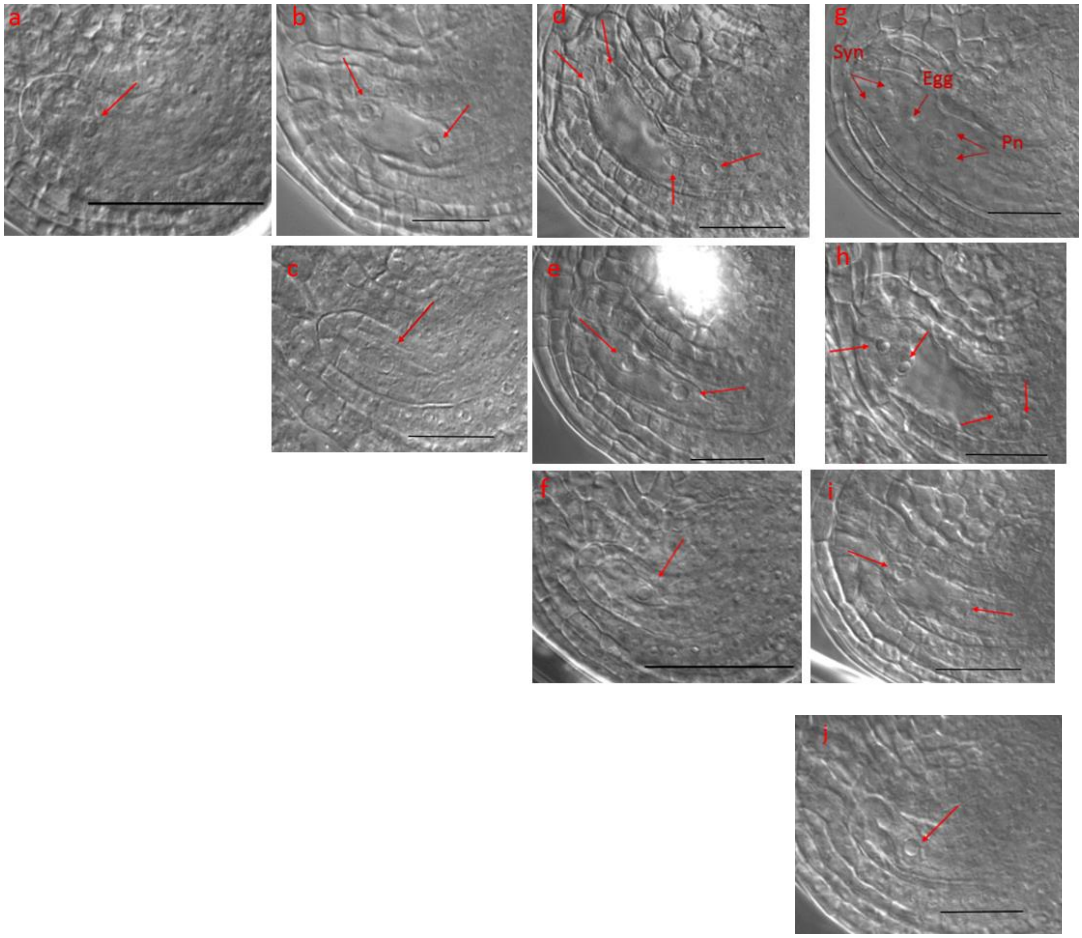

Figure 3.5. The *Atana1* mutation blocks female gametogenesis at different stages

(a, b, d, g) Female gametophytes undergo normal development at one (a), two (b), four (d), eight (g) nucleate stages, and the red arrows are pointing to the nuclei inside of megagametophytes. Figures in the same column show megagametophytes from the same pistil. The ovule in Figure 3.5g shows only five nuclei likely because three antipodal cells can be hardly observed in mature gametophytes.

Syn is short for synergids and Pn is short for Polar nuclei.

The scale bar in each figure represents 50um.

3.2.6 The mutation in *ANA1* leads to programmed cell death of developing seeds and pollen grains

Programmed cell death (PCD) is a self-controlled mechanism through selective elimination of unwanted or damaged cells. Its features include shrinkage of cytoplasm and cleavage of nuclear DNA into oligonucleosomal fragments. And one important modulator of plant PCD is considered to be ROS (Gechev and Hille, 2005; Gadjev et al., 2008).

To reveal whether aborting embryos in the *Atana1-1/+* plants produce an elevated level of ROS, we performed 3,3'-diaminobenzidine (DAB) staining on developing siliques from *Atana1-1/+* and WT to detect hydrogen peroxide (Thordal-Christensen et al., 1997). In WT plants, siliques showed no detectable staining signals (Figure 3.6a). In siliques of *Atana1-1/+*, aborted seeds showed brown color, which indicated a higher level of ROS accumulation (Figure 3.6a and 3.6b).

Apoptotic DNA fragmentation is a key feature of apoptosis, which is a product of endonuclease cleavage of DNA into fragments of 180 base pairs. During apoptosis, the enzyme, caspase activated DNase (CAD), was activated due to cleavage of its inhibitor, inhibitor of caspase activated DNases, by apoptotic effector. The activation of CAD allows DNA in apoptotic cells undergoing enzyme cleavage (Enari et al., 1998). In previous studies, the DNA laddering assay could be an important indicator of apoptosis or programed cell death. Aborting embryos/seeds from the Atana1-1/+ siliques and normally developing

seeds were picked up separately and were extracted for genomic DNA. The genomic DNA from the Atana1-1/+ showed oligonucleosomal (~180bp) DNA ladders (Figure 3.6c).

During our observation of developmental male gametophytes, the condensed nuclei or degraded nuclei in aborted pollen implied that PCD occurs inside of ana1 pollen (Figure 3.4d and 3.4f). To confirm this, the DNA fragmentation in PCD was also detected by the Terminal Deoxynucleotidyl Transferase dUTP Nick End Labelling (TUNEL) assay, which measures the fragmented DNA by attaching fluorescein-12-dUTP(a) at 3´-OH DNA ends using a terminal deoxynucleotidyl transferase enzyme (rTdT) (Gavrieli et al., 1992). We applied the TUNEL assay on sectioned anthers of both WT and *Atana1-1/+*. The tissues were labelled by two colors. Propidium iodide (PI), showing red, stains both apoptotic and non-apoptotic cells. Fluorescein-12-dUTP incorporation, showing yellow, stains nicked DNA. In the anther of WT, the TUNEL signals were not detected in pollen (Figure 3.6d). In *Atana1-1/+*, the TUNEL signals were observed in some aborted pollen grains (Figure 3.6e), indicating that some pollen grains in *Atana1-1/+* underwent PCD.

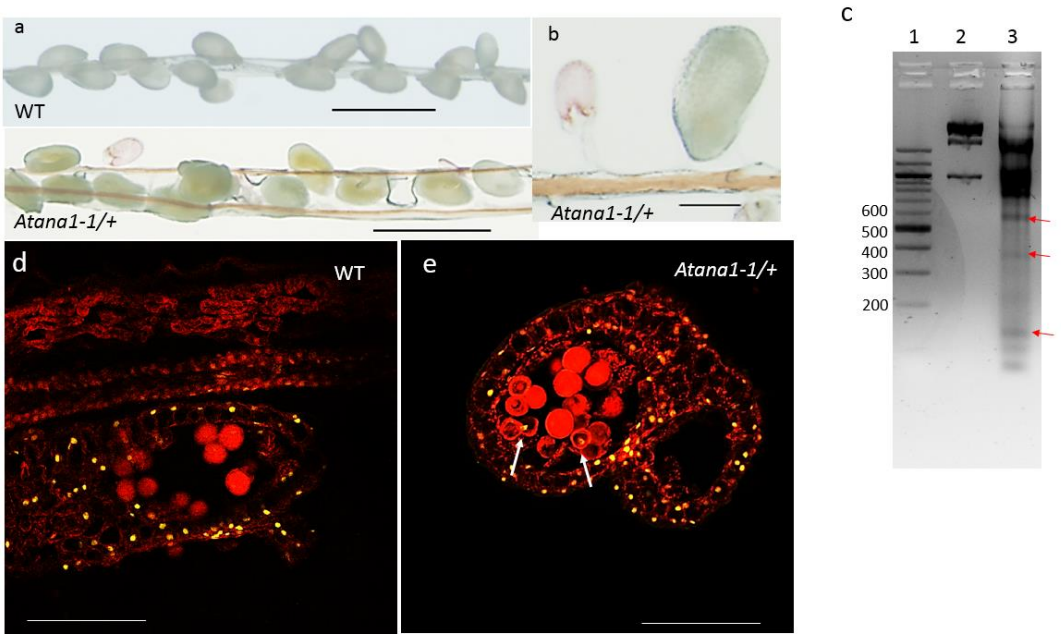

Figure 3.6. Hallmarks of Program cell death (PCD) show in aborted embryos and pollen.

(a) DAB stained siliques of WT and the *Atana1-1/+* self-pollinated plants. The aborted embryos show dark brown in color.

(b) Portion of DAB stained siliques from the *Atana1-1/+* self-pollinated plants.

(c) Lane 1 is markers, Lane 2 shows genomics DNA and RNA from WT, which shows only three ladders and no oligonucleosonal ladders. Lane 3 shows genomic DNA and RNA from the *Atana1* seeds with oligonucleosomal DNA ladders (180bp, 360bp, 540bp). The red arrows are pointing to the oligonucleosomal DNA ladders in *Atana1* seeds.

(d and e) TUNEL assay results of sectioned anthers from both WT and the *Atana1-1/+* plants. Propidium iodide (PI), showing red, stains all cells and fluorescein-12-dUTP incorporation, showing yellow, stains nicked DNA in the nuclei. The white arrows in 3.6e point to pollen grains with TUNEL signals.

Scale bars represent 1mm in 3.6a, 125 um in 3.6b, 75um in 3.6d and 3.6e.

3.2.7 The phenotypes associated with the ana1 mutation can be complemented by the AtANA1 gene

To confirm the abortion of embryogenesis and disruption of gametogenesis were caused by the *Atana1* mutation, the genetic complementation was performed. The complementation vector containing the *AtANA1* genomic DNA, 1494bp upstream and 1018bp downstream amplified from WT genomic DNA was transformed into heterozygous *Atana1-1/+* plants. The homozygous *Atana1* plants which carry the transgene were obtained. These lines, *Atana1Comp*, showed no difference with WT, produced normal pollen grains (Figure 3.3a), ovules, and embryos/seeds (Figure 3.1c).

3.2.8 The *ana1-2* mutation does not affect male gametogenesis

The ana1-2 allele carries a T-DNA insertion at the 6th intron of the *AtANA1* gene. It appears to be a weak allele compared with *ana1-1*. However, homozygous plants also cannot be obtained from selfed *Atana1-2/+* lines.

In the *Atana1-2/+* heterozygous plants, the male gametophytes were normal. As the viability staining showed that only 2.2% (34/1509) of pollen were not viable, a rate similar to the wt plants. However, development of female gametophytes and embryos were affected. From observation of opened siliques of *Atana1-2/+*, 9% (48/534) of ovules and 16.1% (86/534) of seeds were found aborted. In the *Atana1-2/+* self-pollinated plants, some mutant embryos were also arrested at the 2nd division of apical cells (Figure 3.7e-f) while other abnormal embryos went beyond normal development process (Figure 3.7g-h). However, approximately

half of ana1-2 embryos went beyond heart stages but with abnormal morphology (Figure 3.7g-h). The phenotypes of *Atana1-2/+* were also genetically complemented by the *AtANA1* complementation transgene.

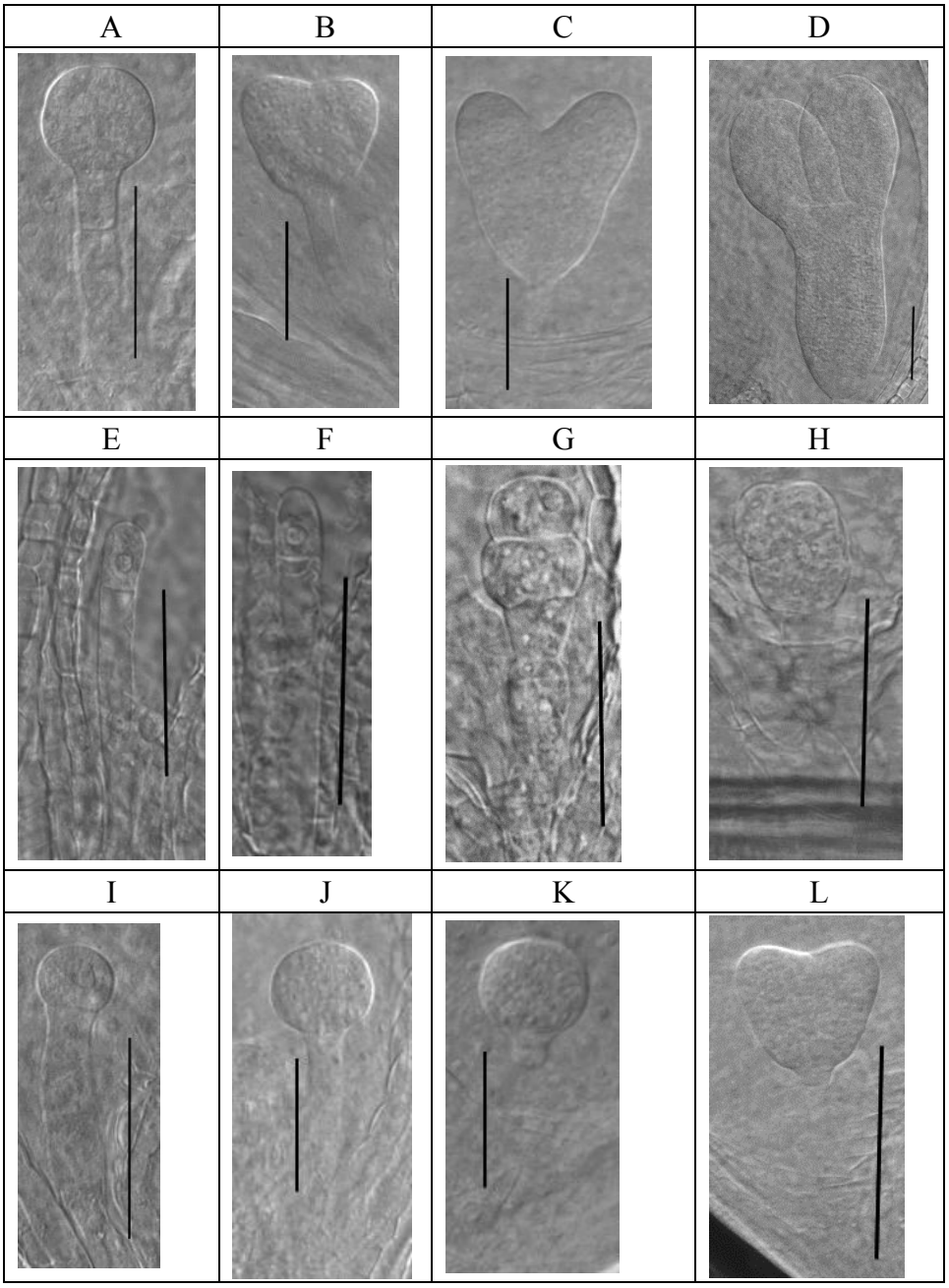

Figure 3.7. Developing embryos from selfed *Atana1-2/+* heterozygous plants shows abnormal embryogenesis

The panels on the same column show embryos from the same silique.

(a, b, c, d) Normal embryos at various developmental stages: globular (a), heart (b) and late heart (c) and linear cotyledon (d) stage.

(e, f) Defective embryos arrested after the first division of zygote.

(g, h) Some embryos show abnormal form.

(i, j, k, l) Embryos show delayed developmental stages comparing to normal embryos in the same silique.

The scale bar represents 50um in each figure.

3.2.9 Expression patterns of *AtANA1*

To investigate the expression patterns of *AtANA1*, a GUS (β-glucuronidase) reporter construct was produced with the *GUS* reporter gene under the control of 1 kb *AtANA1* promoter. Five lines with *AtANA1pro:GUS* transgenic plants were observed, they all showed the similar expression patterns. In floral buds, strong GUS activity was displayed in the floral developmental stages 9-13 (Figure 8a). In the floral buds shown GUS activity, anthers were stained and pollen showed strong GUS activity (Figure 3.8b-c). GUS activity was also detected in peduncles (Figure 8d) and aborted embryos (Figure 3.8e).

3.2.10 AtANA1 protein is localized at cytosol

In order to determine the subcellular localization of AtANA1, an *eYFP* gene was fused at its C terminal with *AtANA1* and the construct under the control of the *35S* promoter was transformed into *Arabidopsis*. The seeding roots of transgenic plants were observed through a confocal fluorescence microscope at 520nm wavelength for detection. The GFP signals in transgenic plants showed that AtANA1 was expressed in the cytosol (Figure 3.9).

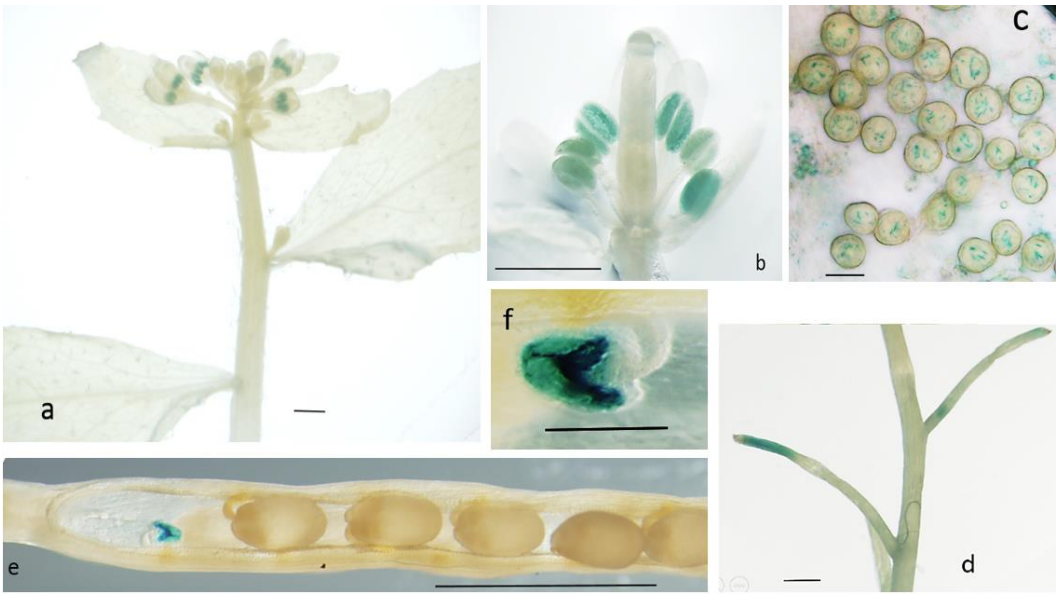

Figure 3.8. Expression patterns of *AtANA1*

AtANA1 expression patterns are exhibited by using the *AtANA1pro:GUS* transgenic plants.

(a-f) GUS staining in inflorescence (a), anthers and pollen (b, c), peduncles (d), and aborted embryos in silique after five days pollination (e and f).

Scale bars in figure 3.7 a, b, d, e and f represent 1mm, and scale bar in 3.7c represents 25um.

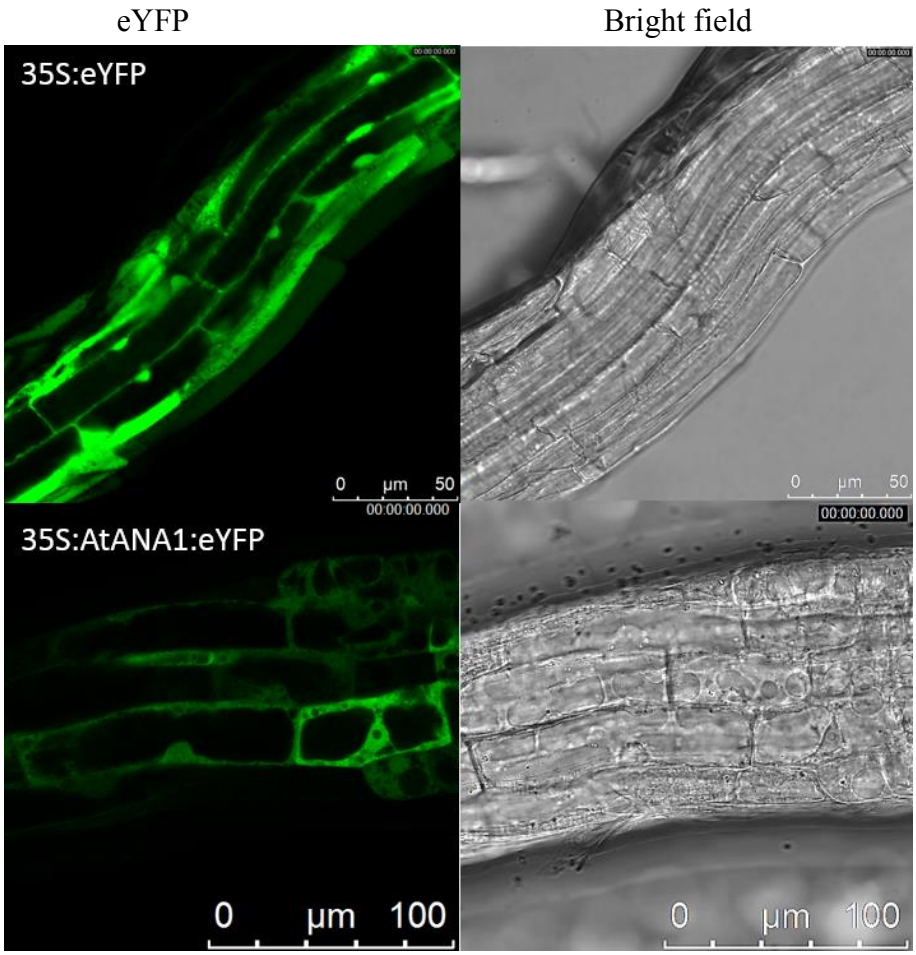

Figure 3.9. AtANA1 is localized in the cytosol.

The eYFP signals in root cells of the *Arabidopsis* with stably expression of the *AtANA1:eYFP* and the *eYFP* were driven by 35s promoter. The fluorescence images and their corresponding bright field images are showed above.

The scale bars with exactly represented length are shown in figures

Chapter Four- AtPUB4 Controls Floral Determinacy

4.1 Introduction

In plants, the shoot apical meristem (SAM) is important for formation of all above-ground organs. Stem cells, localized in the central zone of SAM, can generate different plant organs (Dodsworth, 2009). To maintain activity of the SAM, a homeobox transcription factor, WUSCHEL (WUS) is required. Besides *WUS*, regulation by the *CLAVATA* (*CLV*) pathway is also proved to be essential for maintenance of the SAM. *CLV*-*WUS* forms into a central feedback signal loop. Signals produced by *WUS* expressing cells simulate expression of *CLV3,* and *CLV3*, in turn, functions as a negative signal to depress expression of *WUS* (Fletcher and Meyerowitz, 2000)

In *Arabidopsis*, SAM turns into an inflorescence meristem (IM) during transition from vegetative growth to reproductive growth. Then, the floral primordia outgrow from lateral meristem of IM and continue to emerge and differentiate from the outgrown auxiliary shoot. Floral Meristem (FM) activities are well regulated by bunches of transcription factors to ensure floral identity.

Maintenance of the FM also requires an important transcription factor, *WUS*. Its transcription should be repressed when full set of floral organs have been initiated. The termination timing of the floral meristem is controlled by homeotic MADS-box gene, *AGAMOUS (AG)*. *AG* expression is induced by *WUS* at stage 3 of flower developing (stages according to (Smyth et al., 1990)). At stage 6, *AG* suppresses *WUS* through directly inducing transcription of *KNUCKLES* (*KNU*)

(Sun et al., 2009). Recently, *AG* is also considered to be a direct repressor of *WUS* by directly binding to *WUS* locus and accumulating Polycomb Group (PcG) proteins on *WUS* at stages 4-5 (Liu et al., 2011).

Cells from FM will form four whorls which develop into: sepals, petals, stamens and gynoecia, respectively (Irish, 2010). Stamens, the male reproductive system, contain of anthers and filaments. Development of anther is divided into 13 stages according to morphological landmarks (Sanders et al., 1999). At stage 1, the stamen primordium is formed. During stages 2 to 5, each layer undergoes differentiation and results in four lobes. Meanwhile, archeporial cells differentiated from L2 cells develop into microspore mother cells, which are enclosed by four somatic layers in each lobe from surface to interior: the epidermis, the endothecium, the middle layer, and the tapetum. During male gametogenesis, tapetum protects gametophytes and provides nutrients during the gametogenesis. During stages 10 to 11, tapetal cells undergo programmed cell death and at stage 12, the tapetum layer is almost degenerated. At stage13, anthers undergo dehiscence to facilitate release of pollen grains (Ma, 2005).

Many biological processes in plant, such as pathogen defenses, are controlled by regulation of protein stability. Those biological processes are carried out mainly by ubiquitin-mediated protein degradation pathways. In these pathways, targeted proteins are attached with ubiquitin tag and delivered to 26S proteasomes for degradation. Ubiquitination can also change conformation and activity of proteins. During the ubiquitination process, ubiquitins are first activated by a

ubiquitin activity enzyme (E1) with ATP. The ubiquitins bind to the E1 through a thioester linkage. Then, ubiquitin tag is transferred from the E1 to a ubiquitin conjugating enzyme (E2) and binds to the active site cysteine. The final step requires a ubiquitin protein ligase (E3), which works in targeting the substrate protein and connecting the E2 ligase with the target protein. Majority of E3 ligase proteins contain either a HECT domain or a RING/U–box domain (Moon et al., 2004). The Plant-U-Box (PUB) proteins belong to the U-box domain E3 ligase family. In the *Arabidopsis*, 64 PUB proteins were identified, which are involved in many basic biological processes in plants (Mudgil et al., 2004). For instance, AtPUB17, like its homolog ACR276 in the *Nicotiana tabacum* (tobacco), functions as positive regulators in cell death and defense (Yang et al., 2006). AtPUBc12 and AtPUB13 work on flagellin FLS2 triggered immune responses by targeting the *Arabidopsis* pattern recognition receptor, FLS2, for degradation (Lu et al., 2011). Our interested protein, AtPUB4 made up of 829 amino acids contains a U box and five ARM repeats.

In plants, heterotrimeric GTP-binding proteins consist of Gα,Gβ, and Gγ subunits, which play important roles in transducing extracellular signals by cell surface receptors into intracellular physiological pathways (Neer, 1995). In addition to a single canonical Gα, *Arabidopsis* has three unique Gα-like proteins, XLG1, XLG2, and XLG3 (Ding et al., 2008). In addition to a C terminus that shares sequence similarity with a canonical Gα, XLG proteins also have N terminuses with approximately 400 amino acids that share no significant sequence

similarity with other proteins. In previous study, AtPUB4 was identified to interact with XLGs, which were found to be functional in defense responses.

The *pub4* mutant was not found to have any effects on disease resistance. However, mutation of pub4 was found to cause male sterility due to failure of pollen release, which is caused by enlargement of tapetal cells and incomplete tapetum degeneration. The male sterility trait of the *pub4* mutant is temperature sensitive. At 16^{o}C, a small portion of pollen grains can be released from anther (Wang et al., 2013).

In addition to its role in tapetum development, PUB4 is also involved in regulating floral meristem determinacy. This chapter describes our findings in understanding the role of PUB4 in the floral meristem determinacy. Besides, the chapter also includes the finding that the XLG proteins are also involved in regulating tapetum development.

4.2 Results

4.2.1 PUB4 regulates floral meristem determinacy.

An *Arabidopsis* gynoecium normally contains two fused carpels with four rows of ovules initiated from replums. After fertilization, each ovule develops into a seed and the gynoecium is termed a silique (The seed pod).

The *pub4* mutant produces few seeds under normal growth conditions due to conditional male sterility (Figure 4a). In addition abnormal gynoecia/siliques are often associated with the *pub4* mutant. The abnormal morphology includes different structural features but is typically due to formation of extra floral organs, particularly in upper parts of inflorescences during late developmental stages. Abnormal morphology includes formation of multiple gynoecia on a single receptacle and twisted siliques (Fig 4.1b-4.1c). Some siliques are thicker than normal siliques and are sometimes branched likely due to formation of extra carpel tissues (Fig 4.1d). Extra rows of ovules were formed not only from replums but also on the other interior sides of carpels (Fig 4.1e).

Besides the above observed abnormal features, a more commonly observed abnormal phenomenon is that a fraction of unfertilized *pub4* flowers gave rise to short, kinked, and bulged siliques (Figure 4.2a). These bulged siliques were also mainly formed from flowers on the top of inflorescences in old plants. Further examination revealed that those bulges were caused by growth of extra floral organs inside of carpels. Those ectopic floral organs were formed from placental tissues in the lower half of replums, and were often enclosed within the primary

carpels (Fig 4.2b-4.2c). They underwent senesced and became desiccated when the siliques turned yellow and desiccated (Fig 4.2d). Occasionally, primary carpels ruptured and ectopic floral structures grew out of primary carpels (Fig 4.2e-4.2h). Extra carpelloids might be able to stay green and maintain growth after the primary carpels already turned desiccated. Formation of extra floral organ might show a reiterating pattern with new organs forming from preceding carpel-like structures (Fig 4.2e). The extra carpelloids were often unfused and might have a single or multiple valves with often unsealed replums (Fig 4.2f-4.2g). The ectopic floral organs were generally carpel-like organs, but occasionally, stamens were found inside of primary carpels (Fig 4.2h). However, we have not observed stamen from inside of ectopic carpels.

We excised ectopic carpel-like structures when they were still green and placed them on agar plates containing MS basal salts and 2% sucrose with no hormone added. On the medium, they were able to sustain growth for a longer period and showed a more pronounced reiterating pattern of ectopic floral tissue formation (Fig 4.3a-4.3b). At least four iterations of carpelloids were observed from preceding carpelloids (Figure 4.3b). In addition, the ectopic carpel tissues could also form callus-like tissues which differentiated into multiple carpelloids.

Figure 4.1. Mutation of the *PUB4* causes abnormal gynoecia/siliques

(a) Inflorescences of WT, *pub4* and *pub4 Comp*

(b) Multiple gynoecia are formed on a single receptacle of the *pub4* mutant.

(c) The twisted siliques grow on a single receptacle of *pub4*

(d) A representative thicker silique of *pub4* contains of branched carpel like tissues.

(e) Extra rows of ovules are formed on interior sides of *pub4* primary carpels.

Scar bars in Figure 4.1a, 4.1b and 4.1c represent 1mm, in Figure 4.1d and 4.1e represent 500um

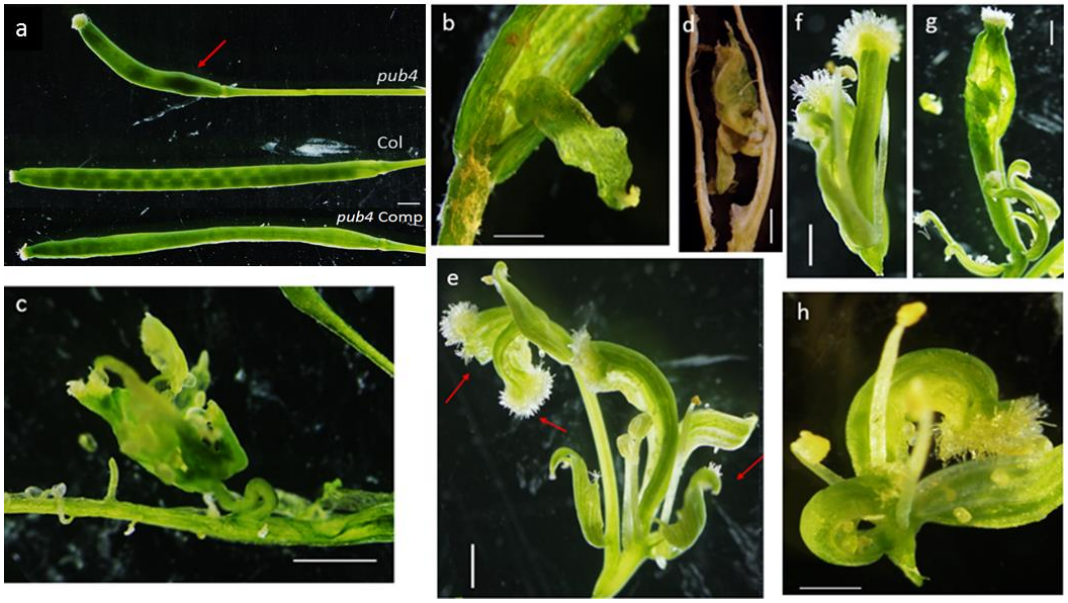

Figure 4.2. The mutation in *PUB4* causes formation of ectopic floral organs insilde of gynoecia/siliques

(a) Siliques of *pub4*, wild type and *pub4Comp*, the silique of *pub4* gives rise to a kinked silique. The red arrow is pointing to bulged part of the silique

(b) The ectopic floral organs in *pub4* are formed at the lower half of primer carpels.

(c) Ectopic floral organs are initiated from replums in the *pub4* plants

(d) The extra carpelloids of *pub4* remain green while primary carpels turn desiccated.

(e) Extra floral organs in *pub4* reiterate formation of carpel-like structures. Red arrows are pointing to ruptured carpels.

(f and g) The extra carpelloids of *pub4* show unfused with a single or multiple valves.

(h) Stamens are also formed inside some of *pub4* primary carpels.

Scale bars in Figure 4.2a, 4.2c , 4.2d, 4.2e, 4.2f and 4.2g represent 1mm and in Figure 4.2b and 4.2h represent 500um.

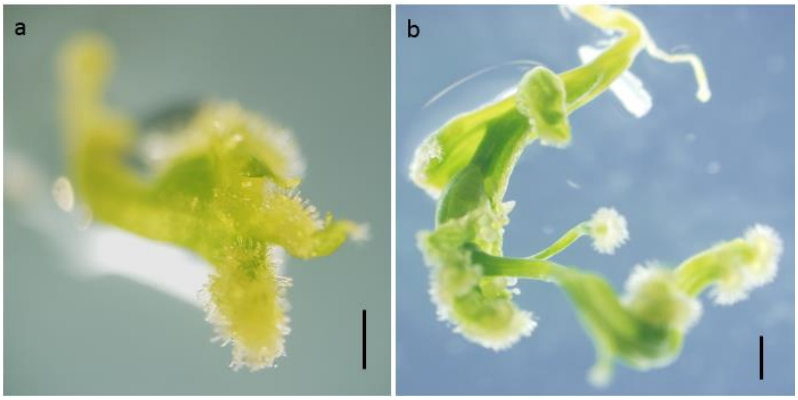

Figure 4.3. The ectopic carpel like structures in *pub4* sustain growing *in vitro*

(a) The excised ectopic carpel-like organs in *pub4* at Day 2 on MS plate

(b) The ectopic carpel-like structures show a reiterating pattern of ectopic floral tissue formation after 6 days growing

Scar bars in Figure 4.3a and 4.3b represent 1mm.

4.2.2 Does auxin plays a role in the PUB4-mediated floral meristem determinacy?

Hormones play important roles in flower and fruit development. Previously, auxin was reported to mark the floral meristem initiation sites and be required for floral organ development (Sundberg and Ostergaard, 2009). Besides, auxin also regulates development of stamens, especially in anther dehiscence (Sundberg and Ostergaard, 2009).

In order to know whether floral meristem indeterminacy in *pub4* is caused by abnormal accumulation of auxin or abnormal auxin response, we introduced the *DR5::GUS* reporter gene into the *pub4* plants and compared expression patterns of the reporter gene in the mutant and wild type plants. The promoter, DR5, contains an auxin-responsive DNA sequence (Ulmasov et al., 1997). The DR5::GUS expression patterns were examined by histochemical staining for GUS activity. According to the GUS staining results, WT showed stronger GUS signals in anthers (Figure 4.4a), in leaves (Figure 4.4b) as well as in embryos inside of siliques (Figure 4.4c and 4.4d). However, GUS signals in *pub4* were reduced comparing to that in WT. It showed little GUS signal in anther (Figure 4.4e and 4.4g) and slight signals at the edge of leaves (Figure 4.4f). Besides, there is no GUS signals detected in siliques of *pub4* (Figure 4.4j). The down-regulated *DR5:GUS* transcription level in *pub4* indicates that mutation of *PUB4* reduced auxin level in plant tissue. However, the role of auxin in modulating PUB4-mediated floral meristem determinacy is yet to be understood.

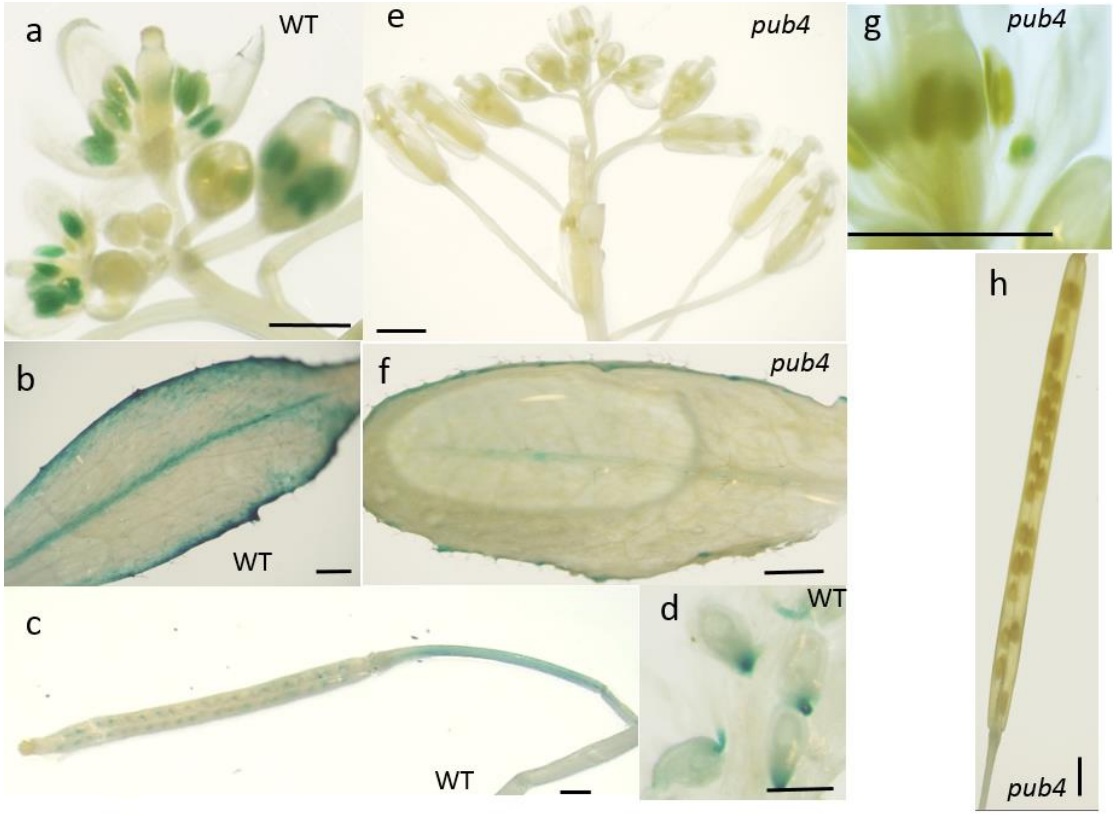

Figure 4.4. Expression patterns of *DR5:GUS* in WT and *pub4*

(a) wildtype flowers showing GUS staining.

(b) A wildtype leaf showing GUS staining.

(c) A wt silique showing GUS staining.

(d) Develping seeds of *pDR5:GUS* transgenic WT plants show GUS signals at the basal part.

(e) GUS staining in *pub4* flowers.

(f) GUS staining in a *pub4* leaf.

(g) Porton of GUS stained pub4 flowers

(h) GUS staining in a *pub4* silique

Scale bars in Figure 4.4a, 4.4b ,4.4c, 4.4e, 4.4f, 4.4g, 4.4h and 4.4j represent 1mm and in Figure 4.4d represents 125um.

4.2.3 *AtPUB4* is involved in controlling pathways of floral stem cells maintenance.

To understand how disruption of *AtPUB4* causes ectopic floral organs growth, we then examined the transcription changes of genes, which are involved in floral determinacy. We compared the mRNA transcription levels of *CLV3*, *WUS*, *AG*, and *KNU* in different organs of *pub4* and WT. In the opening flowers, the mRNA transcription levels of *CLV3* and *WUS* showed slight decrease in *pub4*. (Figure 4.5a). In floral meristem, transcription level of *CLV3* in *pub4* was twice higher than in that in WT (Figure 4.5b). In siliques containing ectopic floral organs, relative mRNA transcription levels of *CLV3*, *WUS* and *AG* were significantly elevated while transcription level of *KNU* was decreased (Figure 4.5c). In the *pub4* plants, the opening flowers and the floral meristem show slight reduction of *WUS* transcription while *WUS* expression level in siliques was significantly up-regulated. We suppose that abnormality of ectopic floral organs growth inside of silique is due to fail of repressing WUS expression. The elevated expression level of *CLV3* may due to continuous activation by *WUS*, but the repression signals from *CLV3* were not workable on *WUS*. It implies that defect of *PUB4* blocks signals from *WUS* negative regulation genes in repressing *WUS* expression. According to our results, no significant changes of *KNU* transcription level showed in flowers and buds while the transcription level of *KNU* is reduced in siliques. Since mutation of *KNU* shows knuckled siliques containing ectopic floral organs inside and male sterility (Payne et al., 2004). The results rises a possibility

that feature in the *pub4* is related to disruption of *KNU*.

a

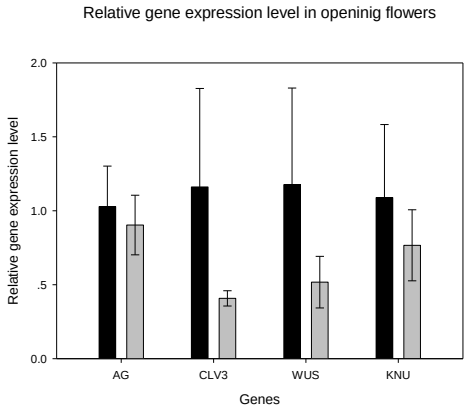

b

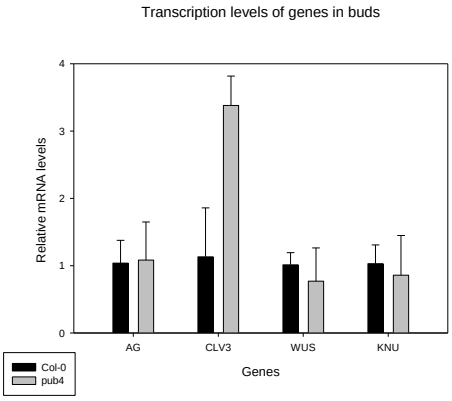

c

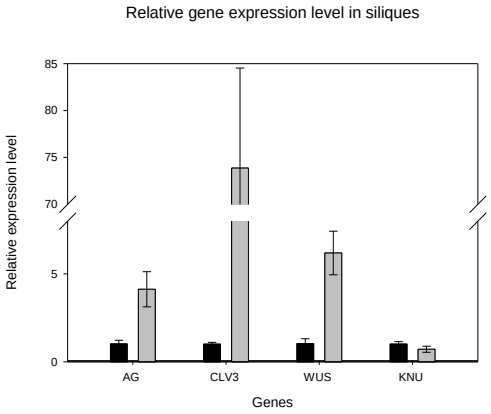

Figure 4.5. Quantitative measurements of gene expression levels in different organs

(a) Comparison of *AG*, *CLV3*, *WUS* and *KNU* mRNA levels in *pub4* opening flowers with that in WT.

(b) Comparison of *AG*, *CLV3*, *WUS* and *KNU* mRNA levels in *pub4* buds with that in WT.

(c) Comparison of *AG*, *CLV3*, *WUS* and *KNU* mRNA levels in *pub4* siliques containing ectopic floral organs with WT siliques.

Real-time RT-PCR performed to examine the levels of *AG*, *CLV*, *WUS*, and *KNU* transcripts used *Actin2* as the internal control. The black bars represent transcript levels in WT and grey bars represent transcript levels in *pub4*.

Error bars represent SD, which were calculated from four biological repeats.

4.2.4 The *pub4* mutation causes ectopic expression of *WUSCHEL* in siliques

To further reveal the alteration of WUS expression caused by the *pub4* mutation, we introduced the *WUSpromoter::GUS* reporter construct into the *pub4* mutant by crossing *pub4* with *WUSpromoter::GUS* transgenetic plants which was previously reported (Liu et al., 2011). In wild type plants, *WUS* expression can be detected at early stage in the floral meristem from stages 1 to 6. Like the results from the qPCR analysis, GUS staining did not show much significant changes of *WUS* expression in floral meristem between *pub4* and WT (Figure 4.6a and 4.6b). In wild type siliques, there were no GUS signals detected in both seeds or in un-pollinated ovules (Figure 4.6c and 4.6d). In *pub4* siliques containing ectopic floral organs, strong GUS signals were detected, especially at the replums (Figure 4.6e and 4.6f). Besides, in *pub4* siliques, the unfertilized ovules showed GUS signals on the basal part of ovule wall (Figure 4.6g and 4.6h). The expression patterns of *WUS* shown in ectopic organs could be the cause of ectopic floral organ formation in *pub4*.

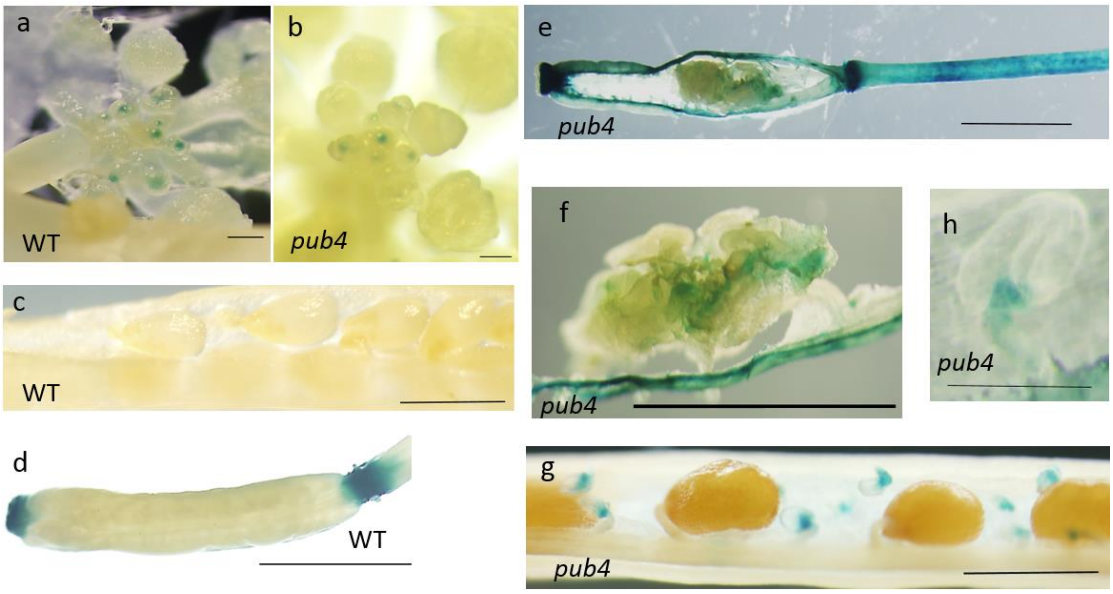

Figure 4.6. Abnormal expression patterns of *WUS* in *pub4* siliques.

(a and b) *WUSpromoter::GUS* expression in flowers of WT (a) and *pub4* (b).

(c) A silique from *WUSprompter::GUS* WT shows no GUS staining signal.

(d) An unpollinated silique of *WUSpromoter::GUS* transgenic plant exhibits no GUS signal

(e and f) A *pub4* silique showing ectopic expression of the reporter in the placental tissues and in the ectopic floral tissue.

(g) A representive silique of *pWUS:GUS* transgenic *pub4* shows strong GUS staining in aborting ovules.

(h) An unpollinated ovule from *pWUS:GUS* transgenetic *pub4* shows GUS staining.

Scale bars in Figure 4.6a , 4.6b and 4.6h represent 125um, in Figure 4.6c and 4.6g represent 500um, in Figure 4.6d , 4.6e and 4.6f represent 1mm .

4.2.5 *AtPUB4* and *AG* act additively in controlling floral meristem determinacy

AGAMOUS (AG) is one of the important negative regulators of *WUS* in floral meristem and the *ag* mutation also leads to a flower-in-flower phenotype (Ji et al., 2011). To reveal the relationship between AG and PUB4 in controlling floral meristem determinacy, we crossed the *pub4* mutant with the *ag10* mutant, which is a weak *agamous* allele (Ji et al., 2011). In the background of the Ler ecotype, some of *ag10* siliques were bulged (20.66%) due to ectopic floral organs inside siliques; however, the *ag10* mutant in the Col-0 ecotype background exhibits little ectopic floral organ formation.

The phenotypic difference of *ag10* in Col and Ler backgrounds indicates presence of a modifier of the *ag10* mutation in the Col-0 ecotype (Liu et al., 2011). The *pub4* mutant is in the Col-0 ecotype background and a small fraction of its siliques (approximately 7.5%) contain ectopic floral organs, mainly in siliques from flowers that formed at a late reproductive stage. We crossed *pub4* with Ler plants and the resulting F1 plants were backcrossed to Ler for four more generations before they were self-crossed. However, the resulting pub4 plants did not show a significant change in the ectopic floral organ phenotype compared with *pub4* in the Col background, suggesting that the modifier of the *ag10* phenotype in Ler does not affect the *pub4* phenotype. The *ag10 pub4* double mutant we generated was in the Col-0 background. Although in the Col background, few *ag10* siliques and a small fraction of *pub10* siliques show

ectopic floral organ formation in siliques, over 90% of siliques in the *ag10 pub4* double mutant were bulged with ectopic floral organs (Figure 4.7a). The above results indicate that *PUB4* and *AG* regulate the floral meristem determinacy through different pathways since the double mutation leads to a much more pronounced defect in terminating floral meristem activity than the single mutation.

The ectopic floral organs in the *ag10pub4* double mutant were further examined under a dissection microscope. Same as in the *pub4* mutant, formation of ectopic floral organs in the *ag10pub4* double mutant gave rise to a knuckle feature to siliques (Figure 4.7b). Other than the much higher frequency of ectopic organ formation, the morphological features of the ectopic floral organs in the double mutant are not significantly different from those in the *pub4* single mutant. However, the ectopic floral organs in siliques of the *ag10pub4* were carpel-like tissues only (Figure 4.7c), which were different from that in *pub4* and $ag10^{Lers}$. The ectopic floral organs in *pub4* contains carpel-like structures or stamen (in the case of *pub4* as described earlier) and so as in $ag10^{lers}$. Majority of ectopic carpels initiated from replums inside of siliques (83.3%) and only a few ectopic carpels in senesced siliques initiated from bottom (16.7%). Similarly, the *WUSpromoter:GUS* line was crossed with the *ag10pub4* double mutant. Strong GUS activity was detected in the placental tissues of siliques in the *WUS promoter::GUS* transgenic *ag10 pub4* lines (Figure 4.7d and 4.7e).

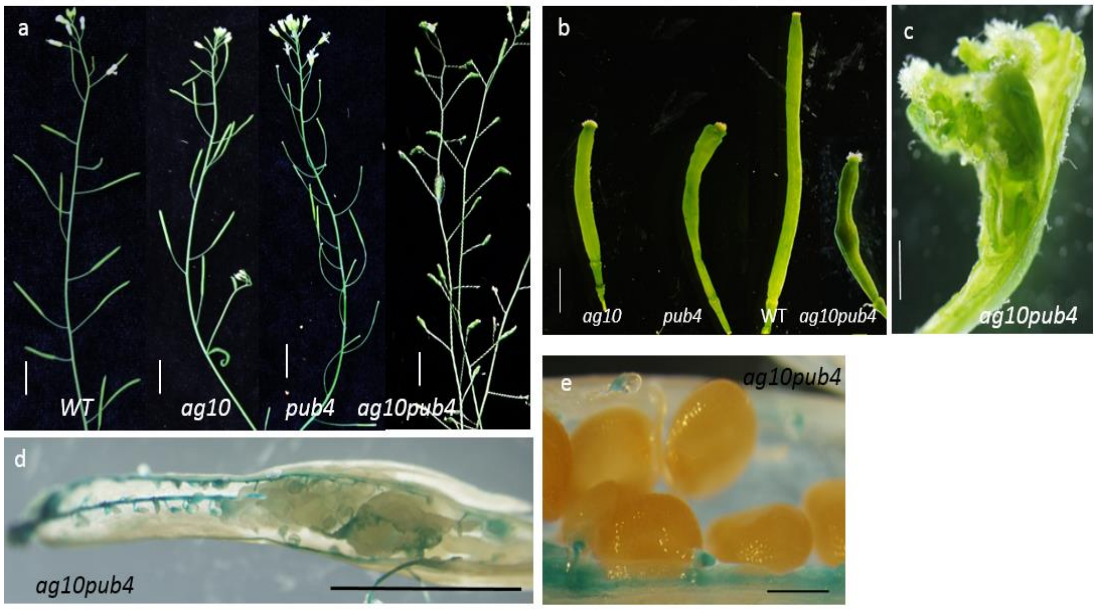

Figure 4.7. The *ag10pub4* double mutant shows enhanced features of ectopic floral organ growth.

(a) Inflorescences of WT, *ag10*, *pub4* and *ag10pub4*.

(b) Siliques of WT, *ag10*, *pub4* and *ag10pub4*

(c) Ectopic carpel organs grow inside of *ag10pub4* primary carpels.

(d) GUS stained silique of *WUS promoter::GUS* transgenic *ag10pub4* shows strong signal in placental tissues

(e) A representive silique of *WUSpromoter:GUS* transgenic *ag10pub4* shows strong GUS staining in aborting ovules.

Scale bar in Figure 4.7a represents 1cm, scale bars in Figure 4.7b and 4.7d represent 1mm, scale bars in Figure 4.7c and 4.7e represent 500um.

4.2.6 PUB4 has E3 ligase activity

PUB4 is predicted to be an E3 ligase with RING-finger/U-box domains. In order to determine whether it indeed possesses an E3 ligase activity, we performed an *in vitro* auto-ubiquitination assay. We expressed and affinity-purified PUB4 protein as a Glutathione S transferase (GST) fusion protein from *Escherichia. coli*. The purified PUB4-GST fusion protein was applied in *in vitro* auto-ubiquitination assay. In this assay E1, E2, FLAG-tagged ubiquitins and ATP were added together with PUB4-GST. This type of E3 ubiquitin ligases are capable of self-ubiquitination in presence of the other components mentioned above. Ubiquitination was detected by Western blotting analysis using the anti-FLAG antibodies. As shown in Fig 4.8 (the second column), PUB4 was attached with ubiquitin-FLAG after the reaction. In absence of PUB4 or another E3 ligase, ubiquitination was not detected. Similarly, if one of the other components (E1, E2, ATP, ubiquitin) was absent, ubiquitination could not occur either. The result indicates that PUB4 is indeed an E3 ligase.

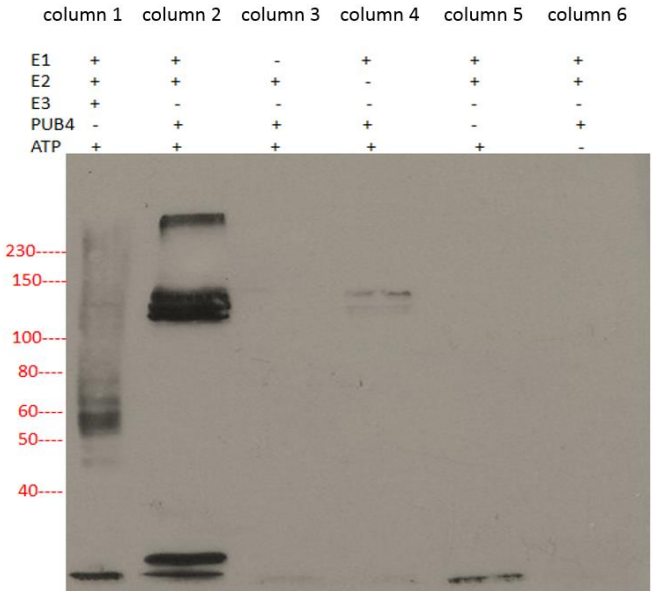

Figure 4.8. PUB4 has an E3 ligase activty

Proteins with ubiquitin-FLAG attached were detected by anti-FLAG antibodies through Western blotting analysis.

The first column shows the result from a positive control, in which a known E3 ligase (His-MurF1, human recombinant 41KDa), human E1 (UBE1), human E2 (Ubc E2), and ATP were added. The detected ladders represent the E3 ligase protein was ubiquitinated.

The second column shows accumulation of ubiquitins over PUB4 (130 KDa), indicating that PUB4 was ubiquitinated.

The Column 3, 4, 5 and 6 all show the negative results, each of them lacked one of the necessary components in the reaction. The presence of two bands at identical sizes (~130 kDa) in column 4 was due to unspecific ubiquitination of PUB4 by UBE1 protein.

4.2.7 AtXLGs, which interact with PUB4, are also involved in regulating growth and degeneration of tapetal cells

In previous study, we identified two Extra-Large G proteins (XLG2 and XLG3) as positive regulators of the defense response in the *Arabidopsis* (Zhu et al., 2009). Through the yeast two hybrid (Y2H) screen, we previously identified PUB2 and PUB4 as putative XLG2 and XLG3 interacting proteins. Moreover, in a separate Y2H screen using PUB4 as the bait, both XLG1 and XLG2 were identified as the PUB4-interacting proteins (Wang et al, unpublished data). However, in the pub4-like phenotype is not associated with any of the *xlg* single mutants, the *xlg2xlg3* double mutant, or the *xlg1xlg2xlg3* triple mutant. The *xlg2* and *xlg3* allele in the *xlg1xlg2xlg3* triple mutant are apparently knock-out allele (Zhu et al., 2009); however, the *xlg1* allele has a T-DNA insertion in its promoter and is likely a weak allele. Later, we obtained another *xlg1* allele (*xlg1-2*) which appears to be a null allele (Wang et al, unpublished data). The *xlg1*-2 shows no discernible phenotype from WT plants. A new triple mutant, *xlg1-2 xlg2 xlg3,* was generated with the *xlg1-2* allele. The triple mutant was found to grow slower than WT plants and, like the *pub4* mutant, is sterile with short and unfertilized siliques (Figure 4.9a and 4.9b).

Further analysis indicates that the sterility is caused by male sterility. The anthers of the *xlg1-2xlg2xlg3* triple mutant were observed through a dissection microscope. Results of Alexander's staining on pollen viability indicated that pollen grains of both the *xlg* triple mutant and *pub4* were viable (Figure 4.9d and

4.9e). However, like *pub4*, pollen looked stuck on the surface of the *xlg1-2xlg2xlg3* mature anthers and failed to be released (Figure 4.9g and 4.9h). The wax sectioning results revealed that the tapetal cells were enlargement at stages 10-11 and failed to be degraded completely at stage 12 (Figure 4.9i). As a result, the pollen grains were attached to the un-degraded tapetal cell residues, which likely is the case of failure in releasing pollen grains from anther (Figure 4.9i). This phenotype caused by the *xlg* triple mutation is identical to that caused by *pub4*, indicating that XLGs play the same roles as PUB4 in controlling of tapetal cell growth and degradation.

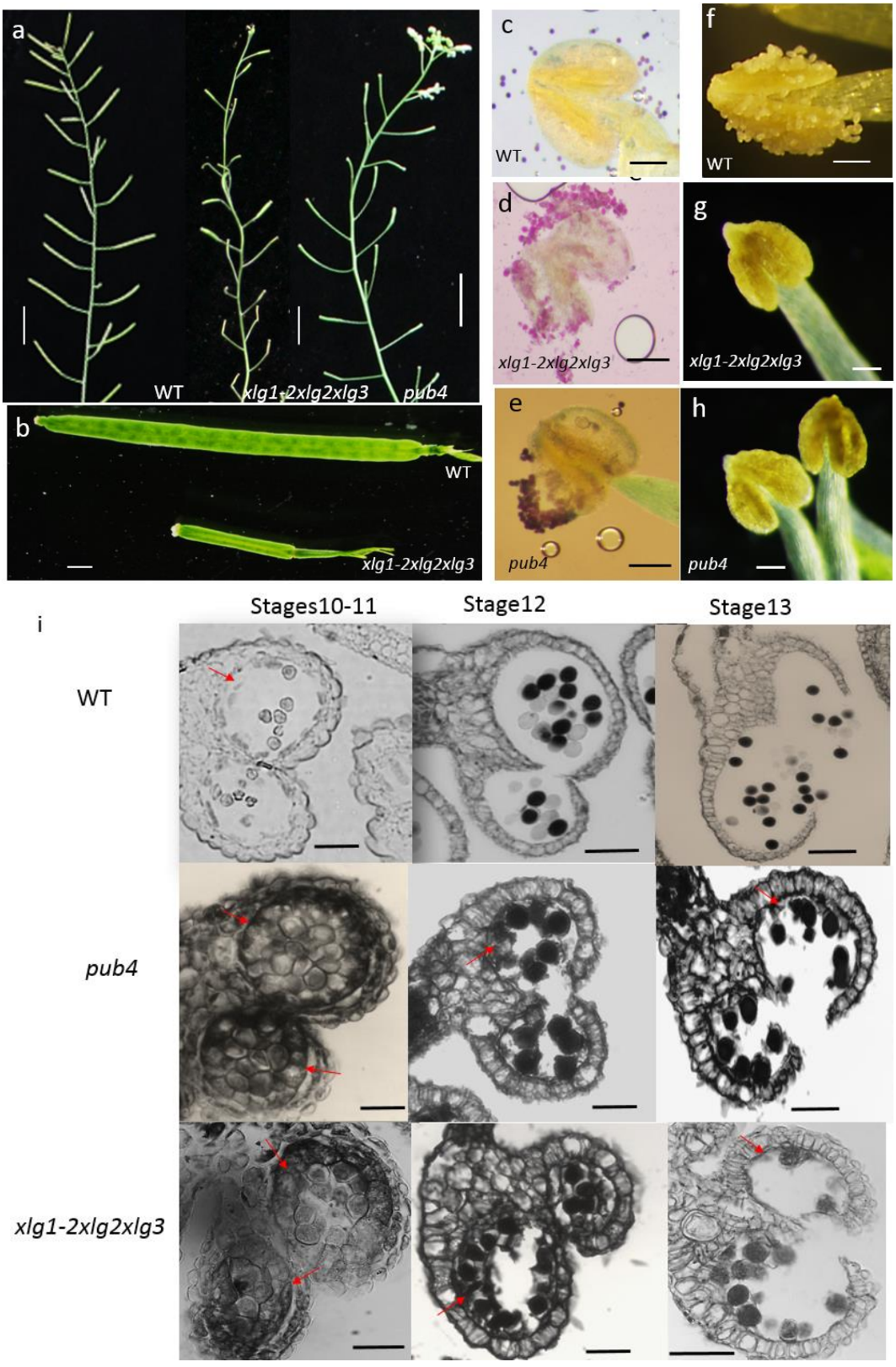

Figure 4.9. The *xlg1-2 xlg2 xlg3* loss-of-function mutant exhibits a similar phenotype as the *pub4* mutant in anther development

(a) Siliques from WT, *xlg1-2xlg2xlg3*, and *pub4*. The *xlg* and *pub4* mutant were

sterile.

(b) A close-up view of a *xlg1-2xlg2xlg3* silique and a WT silique.

(c) The pollen grains produced by WT are viable

(d) The pollen grains produced by *xlg1-2xlg2xlg3* show viability.

(e) The pollen grains produced by *pub4* are viable.

(f) Surface of a WT anther is covered with pollen grains.

(g) Surface of an *xlg1-2xlg2xlg3* anther is smooth and pollen grains hardly released from anther

(h) Surface of a *pub4* anther is smooth and pollen grains hardly released from anther.

(i) Comparison of wax sections of WT, *pub4 and xlg1-2 xlg2 xlg3* anthers.

At stages 10-11, the tapetal cells in WT begin to degenerate while tapetal cells in *pub4* and *xlg1-2xlg2xlg3* are enlarged. The red arrows in Figure 9i are pointing to the tapetal cells. At stage 12, tapetal cells disappear in WT whereas that in *pub4* and *xlg1-2xlg2xlg3* still remain. Pollen grains in *pub4* and *xlg1-2xlg2xlg3* are attached to the undegenerated tapetal cell residues. The red arrows are pointing to un-degraded tapetum layer. At stage13, Pollen grains are releasing from anther when anther dehiscence while pollen grains attached to tapetal cells and fail to release. The red arrows are pointing un-degraded tapetal cell residues.

Scale bar in Figure 4.9a represents 1cm, in Figure 4.9b represents 1mm, in Figure 4.9e-i represent 20um.

Chapter five-Conclusion and Discussion

Flower formation, gametogenesis, fertilization and embryogenesis are essential steps for propagation of flowering plant. Many cellular processes are involved in the gametes development. After gametogenesis completed, eggs are fertilized by pollen. The zygote undergoes embryogenesis, which is a sophisticated process requiring modulation of various hormones. A large number of genes involved in these processes have been identified and studied, but numerous other genes remain to be characterized in those processes.

5.1 AtANA1 is required in gametogenesis and embryogenesis

In this study, the role of AtANA1 in embryogenesis and gametogenesis was characterized. ANA1 was found to be required for embryogenesis and for female and male gametogenesis. The ana1 mutation leads to abortion of embryogenesis at a very early stage. The aborting embryos/seeds exhibited overproduction of ROS and showed DNA fragmentation. Anamorsion was first described in mice as a cytokine-induced anti-apoptotic protein (CIAPIN1) and its over-expression prevents factor-dependent cell lines from withdraw. Knock out of the Anamorsin gene in mice causing embryonic lethality in mice through defective definitive hematopoiesis in liver (Shibayama et al., 2004).

In yeast, the homologous protein of ANA1, DRE2, is also an essential protein. It was reported that Dre2 is a Fe-S containing protein, which plays a role in cytosolic Fe-S protein biogenesis (Zhang et al., 2008). Dre2 forms a complex with

Tah18, diflavin reductase, which is part of an electron transfer chain functioning in the early step of the cytosolic Fe/S protein biogenesis (Netz et al., 2010). In plants, AtANA1 was also considered to form a complex with AtTAH18 and functions in cytosolic iron–sulfur protein assembly (CIA) pathway in electron transferring chain in Arabidopsis (Bernard et al., 2013). AtANA1 was previously identified as a redox-sensitive protein which underwent oxidative modification in *Arabidopsis* cells subjected to the treatment with hydrogen peroxide, Flg22, and SA (Wang et al., 2012). AtANA1 could have a role in ROS signaling pathway and its mutation impairs the oxidative stress response, leading to defects in embryogenesis and gametogenesis.

Recently, the role of AtANA1, named as AtDRE2, was described in epigenetic aspects. The iron-sulfur (Fe-S) cluster is a cofactor of DEMETER, the DNA glycosylase excising 5-methylcytosine via the base excision repair pathway in the central cell before fertilization, which functions as a DNA methylation activator of endosperm lineage (EDL) genes in central cells (Buzas et al., 2014). DNA methylation and demethylation processes were essential for plant reproductive system. During plant life cycle, after zygote undergoing several cell divisions, the DNA in each cell should be modified by methylation to allow cell differentiation. However, during reproductive process, the methylated DNA should undergo demethylation to allow DNA replication. Defect of ANA1 would block the reproductive process in plant life cycle. This could be an explanation how its mutation causes defective embryogenesis and gametogenesis.

Besides impairing embryo development, some *ana1* pollen grains underwent abortion at an early stage of gametogenesis. Interestingly, some of developing pollen carrying the wild type ANA1 allele, which are enclosed in the same anthers containing the ana1 pollen, also underwent abortion.

The phenomenon raises an intriguing possibility that the aborting ana1 pollen might release a death signal that causes neighboring wild type to undergo abortion. However, we could not rule out a possibility that the heterozygous Ana1/ana1 maternal tissues might be the cause of pollen abortion. If so, the ana1 pollen is apparently more sensitive to the unknown death factor from the maternal tissues. Recently, the maternal epigenetic role of ANA1 was also discussed in the newly published article. It is possible that ana1 mutation could be semi-dominant. In this case, the ANA1/ana1 maternal tissue may be the cause of aborting gametes in both male and female. In ANA1-1/+ plant, transcriptional activity of EDL genes in methylation heterozygous maternal tissue was affected (Buzas et al., 2014).

5.2 AtPUB4 regulates floral determinacy as well as development of tapetal cells.

In this study, we found that disruption of *PUB4* causes formation of ectopic floral organs inside of gynoecia/siliques. Ectopic floral organs are formed from placental tissues of siliques. This implies that *PUB4* is required for floral meristem determinacy. Its absence causes placental tissues of gynoecia /siliques to maintain meristematic activity, which leads to uncontrolled cell proliferation and

formation of extra floral organs.

As in normal plants, activity of stem cells in FM and SAM should be terminated to maintain flower determinacy. WUS is the most important transcription factor to maintain activity of stem cells in meristems, regulation of its expression is essential to maintain flower determinacy. Among the regulators of WUS, CLVs form a feedback loop with WUS and produce negative signals to depress expression of WUS. Besides of CLV, AG is also an important inhibitor of WUS during flower development. It directly represses and indirectly represses the expression of WUS.

WUSCHEL (WUS) is required for cell proliferation to maintain SAM and IM. It was found that the *WUS* transcripts were elevated in *pub4* siliques containing ectopic floral organs compared to the WT plants. The abnormal expression of *WUS* in *pub4* siliques was further confirmed by using the *WUSpromoter:: GUS* reporter gene assay. In particular, a strong WUSpromoter::GUS activity was detected in placental tissues of siliques, raising a possibility that the formation of ectopic floral organs in the *pub4* mutant is due to the ectopic expression of *WUS*.

One of the most important regulation pathways involving *WUS* is the CLV-WUS central feedback signal loop (Brand et al., 2000). The *CLV2* and the *CLV3* are simulated to express by the *WUS* signals and the CLV3 in turn represses *WUS* expression (Fletcher and Meyerowitz, 2000). However, according to our mRNA transcription results in *pub4*, *CLAVATA3 (CLV3)* showed extremely high expression levels in siliques containing ectopic floral organs while the *WUS*

expression level was also elevated instead of repressed. The high expression level of *CLV3* could be due to continuous stimulation by the *WUS* signals. However, the repression signals to *WUS* produced by *CLV3* may be blocked due to the absence of *PUB4*.

Another important regulator of *WUS* is AGMOUS (AG), which was considered as a *WUS* inhibitor in the floral meristem and it directly represses *WUS* expression. *KNU* is also involved in the AG controlling pathway. KNU is transcriptional activated by AG and directly represses expression of *WUS*. Disruption of *AG* or *KNU* causes additional floral organ grown in siliques. *ag10*, a weak allele of *ag* mutations also causes additional floral organs inside of some siliques in the Ler background (Liu et al., 2011). AG terminates floral stem cell maintenance in *Arabidopsis* by directly repressing WUS through recruitment of Polycomb Group proteins. Interestingly, the mutation of *KNU* leads to a phenotype very similar to that of *pub4*. First all, both *knu* and *pub4* mutants are conditionally male sterile: they both have more severe male sterility at the normal (22^{o}C) temperature but have increased male fertility at a lower temperature. In addition, the *knu* mutant is also defective in pollen releasing. In addition, like pub4, the *knu* mutant also produce ectopic floral organs from placental tissues of gynoecia/siliques (Payne et al., 2004). It remains to be determined whether KNU could be a substrate of PUB4.

In order to know the genetic relationship between *PUB4* and *AG*, we introduced *ag10* mutation into the *pub4* mutant by crossing the $ag10^{col}$ with *pub4*. The

ag10pub4 double mutant showed a large increased number of siliques that produce ectopic floral organ compared to the single mutants. The *ag10* mutant shows no such phenotype in the Col background and the *pub4* mutant only has a small portion of siliques with additional floral organs; however, in the *ag10pub4* mutant, over 90% of siliques have ectopic floral organs. Abnormal expression of *WUS* in siliques was also detected in the *ag10pub4* double mutant. The results indicate that PUB4 and AG play additively in terminating floral meristem activity.

AtPUB2 and AtPUB4 were previously found to interact with AtXLG proteins in the Y2H system. In this study, it was found that the *xlg1-2xlg2xlg3* triple mutant also showed enlargement of tapetal cells as well as the defect in tapetum layer degradation, which are the same phenotype as *pub4*. This implies that XLGs are also involved in controlling tapetal cell growth and degeneration. Whether PUB4 is involved in ubiquitination of XLGs is also under investigation. However, it appears that the *xlg* triple mutant does not show formation of ectopic floral organs, suggesting an additional role of PUB4 compared with XLGs. On the other hand, XLG2 and XLG3 have been found to play a role in disease resistance; however, we have not found evidence showing that PUB4 is also involved in disease resistance.

List of Reference

Aida M, Vernoux T, Furutani M, Traas J, M T (2002) Roles of PIN-FORMED1 and MONOPTEROS in pattern formation of the apical region of the Arabidopsis embryo. Development 129: 3965-3974

Alandete-Saez M, Ron M, McCormick S (2008) GEX3, expressed in the male gametophyte and in the egg cell of Arabidopsis thaliana, is essential for micropylar pollen tube guidance and plays a role during early embryogenesis. Mol Plant 1: 586-598

Alexander MP (1969) Differential staining of aborted and nonaborted pollen. Stain Technol 44: 117-122

Averyanov A (2009) Oxidative burst and plant disease resistance. Front Biosci (Elite Ed) 1: 142-152

Balk J, Leaver CJ, McCabe PF (1999) Translocation of cytochrome c from the mitochondria to the cytosol occurs during heat-induced programmed cell death in cucumber plants. FEBS Lett 463: 151-154

Bao X, Franks RG, Levin JZ, Liu Z (2004) Repression of AGAMOUS by BELLRINGER in floral and inflorescence meristems. Plant Cell 16: 1478-1489

Bernard DG, Netz DJ, Lagny TJ, Pierik AJ, Balk J (2013) Requirements of the cytosolic iron-sulfur cluster assembly pathway in Arabidopsis. Philos Trans R Soc Lond B Biol Sci 368: 20120259

Bhatt AM, Lister C, Page T, Fransz P, Findlay K, Jones GH, Dickinson HG, Dean C (1999) The DIF1 gene of Arabidopsis is required for meiotic chromosome

segregation and belongs to the REC8/RAD21 cohesin gene family. Plant J 19: 463-472

Bomblies K, Dagenais N, Weigel D (1999) Redundant enhancers mediate transcriptional repression of AGAMOUS by APETALA2. Dev Biol 216: 260-264

Borg M, Brownfield L, Twell D (2009) Male gametophyte development: a molecular perspective. J Exp Bot 60: 1465-1478

Bowman JL, Sakai H, Jack T, Weigel D, Mayer U, Meyerowitz EM (1992) SUPERMAN, a regulator of floral homeotic genes in Arabidopsis. Development 114: 599-615

Bowman JL, Smyth DR, Meyerowitz EM (1989) Genes directing flower development in Arabidopsis. Plant Cell 1: 37-52

Bozhkov PV, Filonova LH, Suarez MF (2005) Programmed cell death in plant embryogenesis. Curr Top Dev Biol 67: 135-179

Bradley D, Ratcliffe O, Vincent C, Carpenter R, Coen E (1997) Inflorescence commitment and architecture in Arabidopsis. Science 275: 80-83

Brand U, Fletcher JC, Hobe M, Meyerowitz EM, Simon R (2000) Dependence of stem cell fate in Arabidopsis on a feedback loop regulated by CLV3 activity. Science 289: 617-619

Breuninger H, Rikirsch E, Hermann M, Ueda M, Laux T (2008) Differential expression of WOX genes mediates apical-basal axis formation in the Arabidopsis embryo. Dev Cell 14: 867-876

Busch M, Mayer U, Jurgens G (1996) Molecular analysis of the Arabidopsis

pattern formation of gene GNOM: gene structure and intragenic complementation. Mol Gen Genet 250: 681-691

Buzas DM, Nakamura M, Kinoshita T (2014) Epigenetic role for the conserved Fe-S cluster biogenesis protein AtDRE2 in Arabidopsis thaliana. Proc Natl Acad Sci U S A 111: 13565-13570

Byrne ME, Simorowski J, RA. M (2002) ASYMMETRIC LEAVES1 reveals knox gene redundancy in Arabidopsis. Development 129: 1957-1965

Capron A, Serralbo O, Fulop K, Frugier F, Parmentier Y, Dong A, Lecureuil A, Guerche P, Kondorosi E, Scheres B, Genschik P (2003) The Arabidopsis anaphase-promoting complex or cyclosome: molecular and genetic characterization of the APC2 subunit. Plant Cell 15: 2370-2382

Carles CC, Choffnes-Inada D, Reville K, Lertpiriyapong K, Fletcher JC (2005) ULTRAPETALA1 encodes a SAND domain putative transcriptional regulator that controls shoot and floral meristem activity in Arabidopsis. Development 132: 897-911

Chen YC, McCormick S (1996) sidecar pollen, an Arabidopsis thaliana male gametophytic mutant with aberrant cell divisions during pollen development. Development 122: 3243-3253

Christensen CA (2002) Mitochondrial GFA2 Is Required for Synergid Cell Death in Arabidopsis. The Plant Cell Online 14: 2215-2232

Colombo M, Masiero S, Vanzulli S, Lardelli P, Kater MM, Colombo L (2008) AGL23, a type I MADS-box gene that controls female gametophyte and embryo

development in Arabidopsis. Plant J 54: 1037-1048

Conner J, Liu Z (2000) LEUNIG, a putative transcriptional corepressor that regulates AGAMOUS expression during flower development. Proc Natl Acad Sci U S A 97: 12902-12907

Dievart A (2003) CLAVATA1 Dominant-Negative Alleles Reveal Functional Overlap between Multiple Receptor Kinases That Regulate Meristem and Organ Development. The Plant Cell Online 15: 1198-1211

Ding L, Pandey S, Assmann SM (2008) Arabidopsis extra-large G proteins (XLGs) regulate root morphogenesis. Plant J 53: 248-263

Dodsworth S (2009) A diverse and intricate signalling network regulates stem cell fate in the shoot apical meristem. Dev Biol 336: 1-9

Ebel C, Mariconti L, Gruissem W (2004) Plant retinoblastoma homologues control nuclear proliferation in the female gametophyte. Nature 429: 776-780

Enari M, Sakahira H, Yokoyama H, Okawa K, Iwamatsu A, Nagata S (1998) A caspase-activated DNase that degrades DNA during apoptosis, and its inhibitor ICAD. Nature 391: 43-50

Epple P, Mack AA, Morris VR, Dangl JL (2003) Antagonistic control of oxidative stress-induced cell death in Arabidopsis by two related, plant-specific zinc finger proteins. Proc Natl Acad Sci U S A 100: 6831-6836

Escobar-Restrepo JM, Huck N, Kessler S, Gagliardini V, Gheyselinck J, Yang WC, Grossniklaus U (2007) The FERONIA receptor-like kinase mediates male-female interactions during pollen tube reception. Science 317: 656-660

Favaro R, Pinyopich A, Battaglia R, Kooiker M, Borghi L, Ditta G, Yanofsky MF, Kater MM, Colombo L (2003) MADS-box protein complexes control carpel and ovule development in Arabidopsis. Plant Cell 15: 2603-2611

Fletcher JC, Meyerowitz EM (2000) Cell signaling within the shoot meristem. Curr Opin Plant Biol 3: 23-30

Franks RG, Wang C, Levin JZ, Liu Z (2002) SEUSS, a member of a novel family of plant regulatory proteins, represses floral homeotic gene expression with LEUNIG. Development 129: 253-263

Friml J, Vieten A, Sauer M, Weijers D, Schwarz H, Hamann T, Offringa R, G. J (2003) Efflux-dependent auxin gradients establish the apical-basal axis of Arabidopsis. Nature 426: 147-153

Gadjev I, Stone JM, Gechev TS (2008) Chapter 3: Programmed Cell Death in Plants. 270: 87-144

Gallois JL, Guyon-Debast A, Lecureuil A, Vezon D, Carpentier V, Bonhomme S, Guerche P (2009) The Arabidopsis proteasome RPT5 subunits are essential for gametophyte development and show accession-dependent redundancy. Plant Cell 21: 442-459

Gavrieli Y, Sherman Y, Ben-Sasson SA (1992) Identification of programmed cell death in situ via specific labeling of nuclear DNA fragmentation. J Cell Biol 119: 493-501

Gechev TS, Hille J (2005) Hydrogen peroxide as a signal controlling plant programmed cell death. J Cell Biol 168: 17-20

Ghezzi P (2005) Oxidoreduction of protein thiols in redox regulation. Biochem Soc Trans 33: 1378-1381

Ghezzi P, Bonetto V (2003) Redox proteomics: identification of oxidatively modified proteins. Proteomics 3: 1145-1153

Grelon M, Vezon D, Gendrot G, Pelletier G (2001) AtSPO11-1 is necessary for efficient meiotic recombination in plants. EMBO J 20: 589-600

Hamann T, Mayer U, G. J (1999) The auxin-insensitive bodenlos mutation affects primary root formation and apical-basal patterning in the Arabidopsis embryo. Development 126: 1387-1395

Harada MALWaJJ (1993) Embryogenesis in Higher Plants: An Overview. Plant Cell

Hatsugai N, Kuroyanagi M, Nishimura M, Hara-Nishimura I (2006) A cellular suicide strategy of plants: vacuole-mediated cell death. Apoptosis 11: 905-911

Huala E, Sussex IM (1992) LEAFY Interacts with Floral Homeotic Genes to Regulate Arabidopsis Floral Development. Plant Cell 4: 901-913

Irish VF (2010) The flowering of Arabidopsis flower development. Plant J 61: 1014-1028

Jasinski S, Piazza P, Craft J, Hay A, Woolley L, Rieu I, Phillips A, Hedden P, Tsiantis M (2005) KNOX action in Arabidopsis is mediated by coordinate regulation of cytokinin and gibberellin activities. Curr Biol 15: 1560-1565

Ji L, Liu X, Yan J, Wang W, Yumul RE, Kim YJ, Dinh TT, Liu J, Cui X, Zheng B, Agarwal M, Liu C, Cao X, Tang G, Chen X (2011) ARGONAUTE10 and

ARGONAUTE1 regulate the termination of floral stem cells through two microRNAs in Arabidopsis. PLoS Genet 7: e1001358

Kim HJ, Oh SA, Brownfield L, Hong SH, Ryu H, Hwang I, Twell D, Nam HG (2008) Control of plant germline proliferation by SCF(FBL17) degradation of cell cycle inhibitors. Nature 455: 1134-1137

Kim YS, Kim SG, Lee M, Lee I, Park HY, Seo PJ, Jung JH, Kwon EJ, Suh SW, Paek KH, Park CM (2008) HD-ZIP III activity is modulated by competitive inhibitors via a feedback loop in Arabidopsis shoot apical meristem development. Plant Cell 20: 920-933

Kwee HS, Sundaresan V (2003) The NOMEGA gene required for female gametophyte development encodes the putative APC6/CDC16 component of the Anaphase Promoting Complex in Arabidopsis. Plant J 36: 853-866

Lam E (2005) Vacuolar proteases livening up programmed cell death. Trends Cell Biol 15: 124-127

Lau S, Slane D, Herud O, Kong J, Jurgens G (2012) Early embryogenesis in flowering plants: setting up the basic body pattern. Annu Rev Plant Biol 63: 483-506

Laux T, Mayer KF, Berger J, Jurgens G (1996) The WUSCHEL gene is required for shoot and floral meristem integrity in Arabidopsis. Development 122: 87-96

Lawen A (2003) Apoptosis-an introduction. Bioessays 25: 888-896

Lenhard M, Bohnert A, Jurgens G, Laux T (2001) Termination of stem cell maintenance in Arabidopsis floral meristems by interactions between WUSCHEL

and AGAMOUS. Cell 105: 805-814

Liu J, Qu LJ (2008) Meiotic and mitotic cell cycle mutants involved in gametophyte development in Arabidopsis. Mol Plant 1: 564-574

Liu J, Zhang Y, Qin G, Tsuge T, Sakaguchi N, Luo G, Sun K, Shi D, Aki S, Zheng N, Aoyama T, Oka A, Yang W, Umeda M, Xie Q, Gu H, Qu LJ (2008) Targeted degradation of the cyclin-dependent kinase inhibitor ICK4/KRP6 by RING-type E3 ligases is essential for mitotic cell cycle progression during Arabidopsis gametogenesis. Plant Cell 20: 1538-1554

Liu X, Kim YJ, Muller R, Yumul RE, Liu C, Pan Y, Cao X, Goodrich J, Chen X (2011) AGAMOUS terminates floral stem cell maintenance in Arabidopsis by directly repressing WUSCHEL through recruitment of Polycomb Group proteins. Plant Cell 23: 3654-3670

Lohmann JU, Hong RL, Hobe M, Busch MA, Parcy F, Simon R, Weigel D (2001) A molecular link between stem cell regulation and floral patterning in Arabidopsis. Cell 105: 793-803

Lu D, Lin W, Gao X, Wu S, Cheng C, Avila J, Heese A, Devarenne TP, He P, Shan L (2011) Direct ubiquitination of pattern recognition receptor FLS2 attenuates plant innate immunity. Science 332: 1439-1442

Ma H (2005) Molecular Genetic Analyses of Microsporogenesis and Microgametogenesis in Flowering Plants. Annu. Rev. Plant Biol.

Ma H, dePamphilis C (2000) The ABCs of floral evolution. Cell 101: 5-8

Mandel MA, Yanofsky MF (1995) A gene triggering flower formation in

Arabidopsis. Nature 377: 522-524

Mayer KF, Schoof H, Haecker A, Lenhard M, Jurgens G, Laux T (1998) Role of WUSCHEL in regulating stem cell fate in the Arabidopsis shoot meristem. Cell 95: 805-815

Miao Y, Laun TM, Smykowski A, Zentgraf U (2007) Arabidopsis MEKK1 can take a short cut: it can directly interact with senescence-related WRKY53 transcription factor on the protein level and can bind to its promoter. Plant Mol Biol 65: 63-76

Ming F, Ma H (2009) A terminator of floral stem cells. Genes Dev 23: 1705-1708

Moon H, Lee B, Choi G, Shin D, Prasad DT, Lee O, Kwak SS, Kim DH, Nam J, Bahk J, Hong JC, Lee SY, Cho MJ, Lim CO, Yun DJ (2003) NDP kinase 2 interacts with two oxidative stress-activated MAPKs to regulate cellular redox state and enhances multiple stress tolerance in transgenic plants. Proc Natl Acad Sci U S A 100: 358-363

Moon J, Parry G, Estelle M (2004) The ubiquitin-proteasome pathway and plant development. Plant Cell 16: 3181-3195

Mudgil Y, Shiu SH, Stone SL, Salt JN, Goring DR (2004) A large complement of the predicted Arabidopsis ARM repeat proteins are members of the U-box E3 ubiquitin ligase family. Plant Physiol 134: 59-66

Nakajima K, Sena G, Nawy T, PN B (2001) Intercellular movement of the putative transcription factor SHR in root patterning. Nature 413: 307-311

Neer EJ (1995) Heterotrimeric G proteins: organizers of transmembrane signals.

Cell 80: 249-257

Netz DJ, Stumpfig M, Dore C, Muhlenhoff U, Pierik AJ, Lill R (2010) Tah18 transfers electrons to Dre2 in cytosolic iron-sulfur protein biogenesis. Nat Chem Biol 6: 758-765

Ngo QA, Moore JM, Baskar R, Grossniklaus U, Sundaresan V (2007) Arabidopsis GLAUCE promotes fertilization-independent endosperm development and expression of paternally inherited alleles. Development 134: 4107-4117

Nowack MK, Grini PE, Jakoby MJ, Lafos M, Koncz C, Schnittger A (2006) A positive signal from the fertilization of the egg cell sets off endosperm proliferation in angiosperm embryogenesis. Nat Genet 38: 63-67

Parcy F, Nilsson O, Busch MA, Lee I, Weigel D (1998) A genetic framework for floral patterning. Nature 395: 561-566

Park SK, Rahman D, Oh SA, Twell D (2004) gemini pollen 2, a male and female gametophytic cytokinesis defective mutation. Sex Plant Reprod 17: 63-70

Payne T, Johnson SD, Koltunow AM (2004) KNUCKLES (KNU) encodes a C2H2 zinc-finger protein that regulates development of basal pattern elements of the Arabidopsis gynoecium. Development 131: 3737-3749

Poole LB, Nelson KJ (2008) Discovering mechanisms of signaling-mediated cysteine oxidation. Curr Opin Chem Biol 12: 18-24

Portereiko MF, Lloyd A, Steffen JG, Punwani JA, Otsuga D, Drews GN (2006) AGL80 is required for central cell and endosperm development in Arabidopsis. Plant Cell 18: 1862-1872

Preuss D, Rhee SY, Davis RW (1994) Tetrad analysis possible in Arabidopsis with mutation of the QUARTET (QRT) genes. Science 264: 1458-1460

Punwani JA, Rabiger DS, Drews GN (2007) MYB98 positively regulates a battery of synergid-expressed genes encoding filiform apparatus localized proteins. Plant Cell 19: 2557-2568

Rotman N, Durbarry A, Wardle A, Yang WC, Chaboud A, Faure JE, Berger F, Twell D (2005) A novel class of MYB factors controls sperm-cell formation in plants. Curr Biol 15: 244-248

Sablowski R (2007) Flowering and determinacy in Arabidopsis. J Exp Bot 58: 899-907

Sakamoto T, Kamiya N, Ueguchi-Tanaka M, Iwahori S, M. M (2001) KNOX homeodomain protein directly suppresses the expression of a gibberellin biosynthetic gene in the tobacco shoot apical meristem. Genes & Development 15: 581-590

Sanchez-Moran E, Osman K, Higgins JD, Pradillo M, Cunado N, Jones GH, Franklin FC (2008) ASY1 coordinates early events in the plant meiotic recombination pathway. Cytogenet Genome Res 120: 302-312

Sanders PM, Bui AQ, Weterings K, McIntire KN, Hsu Y-C, Lee PY, Truong MT, Beals TP, Goldberg RB (1999) Anther developmental defects in Arabidopsis thaliana male-sterile mutants. Sex Plant Reprod 11: 297-322

Schiefthaler U, Balasubramanian S, Sieber P, Chevalier D, Wisman E, Schneitz K (1999) Molecular analysis of NOZZLE, a gene involved in pattern formation and

early sporogenesis during sex organ development in Arabidopsis thaliana. Proc Natl Acad Sci U S A 96: 11664-11669

Schlereth A, Moller B, Liu W, Kientz M, Flipse J, Rademacher EH, Schmid M, Jurgens G, Weijers D (2010) MONOPTEROS controls embryonic root initiation by regulating a mobile transcription factor. Nature 464: 913-916

Schoof H, Lenhard M, Haecker A, Mayer KF, Jürgens G, T. L (2000) The stem cell population of Arabidopsis shoot meristems in maintained by a regulatory loop between the CLAVATA and WUSCHEL genes. Cell 100: 635-644

Schrick K, Mayer U, Martin G, Bellini C, Kuhnt C, Schmidt J, G. J (2002) Interactions between sterol biosynthesis genes in embryonic development of Arabidopsis. Plant J 31: 61-73

Shibayama H, Takai E, Matsumura I, Kouno M, Morii E, Kitamura Y, Takeda J, Kanakura Y (2004) Identification of a cytokine-induced antiapoptotic molecule anamorsin essential for definitive hematopoiesis. J Exp Med 199: 581-592

Smyth DR, Bowman JL, Meyerowitz EM (1990) Early flower development in Arabidopsis. Plant Cell 2: 755-767

Soler N, Delagoutte E, Miron S, Facca C, Baille D, d'Autreaux B, Craescu G, Frapart YM, Mansuy D, Baldacci G, Huang ME, Vernis L (2011) Interaction between the reductase Tah18 and highly conserved Fe-S containing Dre2 C-terminus is essential for yeast viability. Mol Microbiol 82: 54-67

Sun B, Xu Y, Ng KH, Ito T (2009) A timing mechanism for stem cell maintenance and differentiation in the Arabidopsis floral meristem. Genes Dev 23: 1791-1804

Sundberg E, Ostergaard L (2009) Distinct and dynamic auxin activities during reproductive development. Cold Spring Harb Perspect Biol 1: a001628

Thordal-Christensen H, Zhang Z, Wei Y, Collinge DB (1997) Subcellular localization of H2O2 in plants. H2O2 accumulation in papillae and hypersensitive response during the barley—powdery mildew interaction. the plant Journal 11: 1187-1194

Twell D, Park SK, Hawkins TJ, Schubert D, Schmidt R, Smertenko A, Hussey PJ (2002) MOR1/GEM1 has an essential role in the plant-specific cytokinetic phragmoplast. Nat Cell Biol 4: 711-714

Ueda M, Zhang Z, Laux T (2011) Transcriptional activation of Arabidopsis axis patterning genes WOX8/9 links zygote polarity to embryo development. Dev Cell 20: 264-270

Ulmasov T, Murfett J, Hagen G, Guilfoyle TJ (1997) Aux/IAA proteins repress expression of reporter genes containing natural and highly active synthetic auxin response elements. Plant Cell 9: 1963-1971

Vernis L, Facca C, Delagoutte E, Soler N, Chanet R, Guiard B, Faye G, Baldacci G (2009) A newly identified essential complex, Dre2-Tah18, controls mitochondria integrity and cell death after oxidative stress in yeast. PLoS One 4: e4376

Wang H, Li J, Bostock RM, Gilchrist DG (1996) Apoptosis: A Functional Paradigm for Programmed Plant Cell Death Induced by a Host-Selective Phytotoxin and Invoked during Development. Plant Cell 8: 375-391

Wang H, Lu Y, Jiang T, Berg H, Li C, Xia Y (2013) The Arabidopsis U-box/ARM repeat E3 ligase AtPUB4 influences growth and degeneration of tapetal cells, and its mutation leads to conditional male sterility. Plant J 74: 511-523

Wang H, Wang S, Lu Y, Alvarez S, Hicks LM, Ge X, Xia Y (2012) Proteomic analysis of early-responsive redox-sensitive proteins in Arabidopsis. J Proteome Res 11: 412-424

West M, Harada JJ (1993) Embryogenesis in Higher Plants: An Overview. Plant Cell 5: 1361-1369

Williams L, Grigg SP, Xie M, Christensen S, Fletcher JC (2005) Regulation of Arabidopsis shoot apical meristem and lateral organ formation by microRNA miR166g and its AtHD-ZIP target genes. Development 132: 3657-3668

Wu X, Dabi T, Weigel D (2005) Requirement of homeobox gene STIMPY/WOX9 for Arabidopsis meristem growth and maintenance. Curr Biol 15: 436-440

Wurschum T, Gross-Hardt R, Laux T (2006) APETALA2 regulates the stem cell niche in the Arabidopsis shoot meristem. Plant Cell 18: 295-307

Yang CW, Gonzalez-Lamothe R, Ewan RA, Rowland O, Yoshioka H, Shenton M, Ye H, O'Donnell E, Jones JD, Sadanandom A (2006) The E3 ubiquitin ligase activity of arabidopsis PLANT U-BOX17 and its functional tobacco homolog ACRE276 are required for cell death and defense. Plant Cell 18: 1084-1098

Yang WC, Shi DQ, Chen YH (2010) Female gametophyte development in flowering plants. Annu Rev Plant Biol 61: 89-108

Yang WC, Ye D, Xu J, Sundaresan V (1999) The SPOROCYTELESS gene of

Arabidopsis is required for initiation of sporogenesis and encodes a novel nuclear protein. Genes Dev 13: 2108-2117

Yu HJ, Hogan P, Sundaresan V (2005) Analysis of the female gametophyte transcriptome of Arabidopsis by comparative expression profiling. Plant Physiol 139: 1853-1869

Yu LP, Miller AK, Clark SE (2003) POLTERGEIST encodes a protein phosphatase 2C that regulates CLAVATA pathways controlling stem cell identity at Arabidopsis shoot and flower meristems. Curr Biol 13: 179-188

Yu LP, Simon EJ, Trotochaud AE, Clark SE (2000) POLTERGEIST functions to regulate meristem development downstream of the CLAVATA loci. Development 127: 1661-1670

Yu XH, Perdue TD, Heimer YM, Jones AM (2002) Mitochondrial involvement in tracheary element programmed cell death. Cell Death Differ 9: 189-198

Zhang Y, Lyver ER, Nakamaru-Ogiso E, Yoon H, Amutha B, Lee DW, Bi E, Ohnishi T, Daldal F, Pain D, Dancis A (2008) Dre2, a conserved eukaryotic Fe/S cluster protein, functions in cytosolic Fe/S protein biogenesis. Mol Cell Biol 28: 5569-5582

Zhao D, Yu Q, Chen M, Ma H (2001) The ASK1 gene regulates B function gene expression in cooperation with UFO and LEAFY in Arabidopsis. Development 128: 2735-2746

Zhu H, Li GJ, Ding L, Cui X, Berg H, Assmann SM, Xia Y (2009) Arabidopsis extra large G-protein 2 (XLG2) interacts with the Gbeta subunit of heterotrimeric

G protein and functions in disease resistance. Mol Plant 2: 513-525

Curriculum Vitae

Academic qualifications of the thesis author, Miss YU Boying:

- Received the degree of Bachelor of Science (Honours) from Hong Kong Baptist University, November 2010.

January 2015